JAERI-M
82-076

A BEST ESTIMATE ANALYSIS OF LOFT L3-6/L8-1 BY RELAP4/MOD6/U4/J3

July 1982

Kazuo FUJIKI and Kazuo YOSHIDA

日本原子力研究所
Japan Atomic Energy Research Institute

JAERI-Mレポートは，日本原子力研究所が不定期に公刊している研究報告書です。
入手の問合わせは，日本原子力研究所技術情報部情報資料課（〒319-11茨城県那珂郡東海村）あて，お申しこしください。なお，このほかに財団法人原子力弘済会資料センター（〒319-11 茨城県那珂郡東海村日本原子力研究所内）で複写による実費頒布をおこなっております。

JAERI-M reports are issued irregularly.
Inquiries about availability of the reports should be addressed to Information Section, Division of Technical Information, Japan Atomic Energy Research Institute, Tokai-mura, Naka-gun, Ibaraki-ken 319-11, Japan.

編集兼発行　日本原子力研究所
印　　刷　いばらき印刷㈱

JAERI-M 82-076

A Best Estimate Analysis of LOFT L3-6/L8-1 by RELAP4/MOD6/U4/J3

Kazuo FUJIKI and Kazuo YOSHIDA

Division of Nuclear Safety Evaluation,
Tokai Research Establishment, JAERI

(Received June 2, 1982)

Thermal-hydraulic analysis of LOCE L3-6/L8-1, which is the one of loss-of-coolant experiments (LOCEs) in the loss-of-fluid test (LOFT) facility, was performed by using RELAP4/MOD6/U4/J3. Main purpose of the analysis is to assess the capability of the RELAP4/MOD6/U4/J3 code upon the analysis of a small break LOCA in a PWR.

The code calculated the thermal-hydraulic behavior in the primary and secondary systems. Calculated results showed good agreement with measured data about break flow, pressure and temperature of the primary system and fluid densities in the in the intact loop, but the behavior of broken loop and steam generator secondary system were not calculated well.

In the course of this analysis, some improvements were found to be necessary on the modeling of pump degradation and coast down, steam generator and stagnant fluid in the broken loop.

Keywords: RELAP4/MOD6/U4/J3, LOFT, PWR, Best Estimate Analysis, Small Break, Thermal-Hydraulic Analysis, Comparative Evaluations, Reactor Safety, Reactor Cooling Systems

JAERI－M　82－076

RELAP4／MOD6／U4／J3によるLOFT L3－6／L8－1実験解析

日本原子力研究所東海研究所安全解析部
藤木　和男・吉田　一雄

（1982年6月2日受理）

米国LOFT原子炉において実施された実験L3－6／L8－1の解析をRELAP4／MOD6／U4／J3コードを用いて行なった。解析の主たる目的はPWRの小口径破断・冷却材喪失事故に対するRELAP4／MOD6／U4／J3コードの解析能力を検証することである。1次冷却系統の圧力，温度，破断口からの放出流量，系内の冷却材分布，燃料棒温度挙動等についてコードによる計算結果と実験データとの比較を行ない，その結果，破断流量，一次系の圧力，温度及びホットレグの分離二相流以外の健全ループ内流動については両者は良い一致を示した。しかしながら主冷却水ポンプの二相流状態での挙動，蒸気発生器，破断ループ（停滞水）に関しては解析モデルの改良が必要なことが明らかになった。

CONTENTS

目　　次

1. Introduction

RELAP4/MOD6/U4/J3 is an improved version of RELAP4/MOD6 so as to extend the code capabilities to analysis of small break LOCA in both a PWR and a BWR. To verify the overall capability of the RELAP4/MOD6/U4/J3 code on the analysis of a small break LOCA in a PWR, the analysis of LOFT Test L3-6/L8-1 was performed by RELAP4/MOD6/U4/J3.

The LOFT facility is a 50 MWt PWR with instrumentation to measure and provide data on the thermal-hydraulic conditions throughout the system. The brief descriptions on the LOFT system is given in Appendix A of this report and detailed informations are described in Reference(7).

Loss-of-Coolant Experiment (LOCE) L3-6/L8-1, which was conducted in the LOFT facility on December 10, 1980, consisted of two parts. Experiment L3-6 was the fifth nuclear experiment in the LOFT Small Break Experiment Series L3 and simulated a 4-in. diameter break in the cold leg of a primary coolant loop of a four-loop commercial PWR. Experiment L8-1 was the first experiment in the LOFT Severe Core Transient Experiment Series L8, in which the liquid in the reactor vessel collapsed to below the lower core elevation.

Prior to performing the analysis, the experimental data report for LOCE L3-6/L8-1 has been distributed, thus the initial conditions and a part of the boundary conditions during transient were determined from the data report. Since RELAP4/MOD6/U4/J3 still includes a thermal equilibrium assumption between phases, some difficulties on the treatment of the ECC mixing problem has been expected to occur when highly subcooled water from ECCS is injected to the system. Based on this aspect, the analysis is focused on the phenomena up to the accumulator and HPIS activation at 2462 seconds. The calculated results and the experimental data show good agreement about the overall primary system behavior, i.e, primary system pressure and mass inventory but slightly different in secondary system behavior. It was also shown that the calculated water distribution in the primary system differed from the experimental data, and this made the start of core uncovery and fuel temperature excursions earlier than the data after PCPs (primary coolant pumps) trip.

Section 2 states the JAERI improved version of the RELAP4/MOD6 code. Section 3 presents the modeling of the LOFT system utilized in the analysis. Section 4 summarized initial conditions used in the anal-

ysis. Section 5 presents the calculated results and the comparison with the experimental data. Conclusions are stated in Section 6. Appendix A describes the LOFT system briefly.

2. Brief Description of RELAP4/MOD6/U4/J3

RELAP4/MOD6/U4/J3 is the latest improved version of RELAP4/MOD6 in JAERI, and includes many modifications and improvements of the model for the analysis of the transient thermal-hydraulic behavior during loss-of-coolant accident in an LWR.

Major improvements are for the analysis of refill and reflood phases of not only large break but also small break LOCA in a BWR. The modifications of the models for a small break analysis already incorporated in the original RELAP4/MOD6 code were also included in our improved version. In the following subsections, the analytical models and unique features of RELAP4/MOD6/U4/J3 relating to the analysis of LOCE L3-6/L8-1 are described briefly.

2.1 Vertical Slip Junction Model

In the vertical slip model used in the original RELAP4/MOD6, the junction void fraction for the estimation of slip velocity is obtained from the quality averaged over the upper and lower control volumes. This method implicity assumes that the phase separation model is not applied to both upper and lower control volumes. In the JAERI improved version, the junction void fraction for the slip verocity calculation is determined from local fluid properties near the junction which are possibly modified by an application of the separation model to the volumes. This approach seems to be physically adequate when the mixture level exists in either the upper or lower control volumes.

2.2 Single Mixture Level Calculation in Vertically Stacked Volumes

The purpose of the single mixture level calculation in vertically stacked volumes is to avoid unrealistic vapor-mixture layering. In the original RELAP4/MOD6, however, the multi-layered vapor-mixture structure can still appear even the index for single level calculation is assigned, because the calculational procedure in the code is inadequate and somewhat mistaken. So the procedure of single level calculation is

ysis. Section 5 presents the calculated results and the comparison with the experimental data. Conclusions are stated in Section 6. Appendix A describes the LOFT system briefly.

2. Brief Description of RELAP4/MOD6/U4/J3

RELAP4/MOD6/U4/J3 is the latest improved version of RELAP4/MOD6 in JAERI, and includes many modifications and improvements of the model for the analysis of the transient thermal-hydraulic behavior during loss-of-coolant accident in an LWR.

Major improvements are for the analysis of refill and reflood phases of not only large break but also small break LOCA in a BWR. The modifications of the models for a small break analysis already incorporated in the original RELAP4/MOD6 code were also included in our improved version. In the following subsections, the analytical models and unique features of RELAP4/MOD6/U4/J3 relating to the analysis of LOCE L3-6/L8-1 are described briefly.

2.1 Vertical Slip Junction Model

In the vertical slip model used in the original RELAP4/MOD6, the junction void fraction for the estimation of slip velocity is obtained from the quality averaged over the upper and lower control volumes. This method implicity assumes that the phase separation model is not applied to both upper and lower control volumes. In the JAERI improved version, the junction void fraction for the slip verocity calculation is determined from local fluid properties near the junction which are possibly modified by an application of the separation model to the volumes. This approach seems to be physically adequate when the mixture level exists in either the upper or lower control volumes.

2.2 Single Mixture Level Calculation in Vertically Stacked Volumes

The purpose of the single mixture level calculation in vertically stacked volumes is to avoid unrealistic vapor-mixture layering. In the original RELAP4/MOD6, however, the multi-layered vapor-mixture structure can still appear even the index for single level calculation is assigned, because the calculational procedure in the code is inadequate and somewhat mistaken. So the procedure of single level calculation is

modified in the JAERI improved version as below.

i) If the mixture level in the upper volume is greater than some small value (0.05 ft is default), only bubble gradient in the mixture is calculated for the lower control volume and the mixture level is set equal to the volume height.

ii) The small value for the level to control the mixture level calculation can be changed, if necessary, to other than 0.05 ft by the input.

In addition to the above, the junction enthalpy is automatically smoothed for the vertical junctions if JVERTL =1 without regarding that upstream and downstream volumes are overlapping or not, whenever mixture level passes the junction elevation point.

2.3 Extended Trip Control Capability

The "trip" in the original RELAP4/MOD6 can control the timing of initiation or termination of the bubble rise model application to specific control volume. In the JAERI improved version, MOD6/U4/J3, the trips are also able to control the application of vertical slip model for specific junctions. It means it is able to apply the slip model for some specific junctions only for the limited intervals.

The trips can be turned off at any time when the reset conditions specified in the Trip Data Cards are satisfied after once they have been turned on. For example, if two set points, one for the signal to open by high-pressure and the other for the signal to close by low pressure, are supplied for the valve action, the specified valve will act cyclic (repeat open/close) according to the change of reference volume pressure.

3. Modeling of the System

A system model for RELAP4/MOD6 described in subsection 3.1 was the modified model developed and reported[4] by INEL for the analysis of LOFT L3 experiments. Modifications on the system model were mainly on the ECCS model, slip and level calculation options. Steam generator secondary model was also slightly changed. These changes are described in the following subsections.

modified in the JAERI improved version as below.

i) If the mixture level in the upper volume is greater than some small value (0.05 ft is default), only bubble gradient in the mixture is calculated for the lower control volume and the mixture level is set equal to the volume height.

ii) The small value for the level to control the mixture level calculation can be changed, if necessary, to other than 0.05 ft by the input.

In addition to the above, the junction enthalpy is automatically smoothed for the vertical junctions if JVERTL =1 without regarding that upstream and downstream volumes are overlapping or not, whenever mixture level passes the junction elevation point.

2.3 Extended Trip Control Capability

The "trip" in the original RELAP4/MOD6 can control the timing of initiation or termination of the bubble rise model application to specific control volume. In the JAERI improved version, MOD6/U4/J3, the trips are also able to control the application of vertical slip model for specific junctions. It means it is able to apply the slip model for some specific junctions only for the limited intervals.

The trips can be turned off at any time when the reset conditions specified in the Trip Data Cards are satisfied after once they have been turned on. For example, if two set points, one for the signal to open by high-pressure and the other for the signal to close by low pressure, are supplied for the valve action, the specified valve will act cyclic (repeat open/close) according to the change of reference volume pressure.

3. Modeling of the System

A system model for RELAP4/MOD6 described in subsection 3.1 was the modified model developed and reported[4] by INEL for the analysis of LOFT L3 experiments. Modifications on the system model were mainly on the ECCS model, slip and level calculation options. Steam generator secondary model was also slightly changed. These changes are described in the following subsections.

3.1 System Nodalization

A schematic of the LOFT system model is given in Figure 3.1. As mentioned above, this model is based on the INEL's model[4] with minor changes. The model consists of 37 control volumes, 47 junctions, and 16 heat slabs. A brief description of each control volume is given in Table 3.1 and of each heat slab is given in Table 3.2. The modifications from the INEL model are;

i) Junction for the break (Junction 45) is located at the intact loop cold leg (Volume 19). Downstream of the break junction is the normal control volume with infinitely large volume.

ii) The modeled ECCS is divided into two groups. One consists of accumulator (Volume 33) and HPIS A (Fill Junction 37), and is injected to the downcomer through the modeled ECC line (Volume 34) (not to the intact cold leg). Another is HPIS B which is directly injected to the intact cold leg (Fill Junction 38).

iii) Two junctions are added to the steam generator secondary model. One normal junction represents the leakage through the steamline control valve and another negative fill junction is for the normal operation actions of steamline control valve.

3.2 Primary Coolant Model

3.2.1 Critical Flow Model

The critical flow model specified for the break junction was the combination of the Henry-Fauske and Homogeneous Equilibrium Model (HEM), which used the extended Henry tables for the subcooled region and with a transition into HEM at 0.02% quality. Multiplier of 0.8 was applied to both the saturated Henry and HEM values.

3.2.2 Slip Model

The vertical slip model of RELAP4/MOD6/U4/J3 was applied to the following junctions after the primary coolant pumps tripped (2371.4 seconds); core inlet through the upper plenum (Junctions 1 through 5), steam generator tubes (Junctiosn 8,9,10,12,13 and 14), and downcomer annulus (Junction 21).

The parameters used in the slip velocity correlation were the default values in the code.

3.2.3 Bubble Rise Model

Mixture level calculations by means of bubble rise model of RELAP4/MOD6 were carried out as follows. The Wilson bubble rise model with ALPH (bubble gradient parameter) = 0.0 was used in;

i) Pressurizer (Volume 32) and Volume 29, but tripped to homogeneous when the level dropped to 0.03 m.

ii) Upper plenum (Volume 5) and steam generator simulator (Volumes 26 and 27) throughout the transient.

iii) Core (Volumes 1 through 4), steam generator (Volumes 8 through 13), intact loop between steam generator and pumps (Volumes 14, 15 and 16), reactor vessel inlet annulus (Volume 20) and the downcomer (Volumes 21 and 22), after the primary coolant pumps tripped.

3.2.4 ECC System Model

The model of the ECCS includes the accumulator injection system and HPIS. The LPIS was ignored because it did not activated in the L3-6 experiment. The HPIS was represented by fill junctions (Junctions 37 and 38, for A and B subsystems, respectively). HPIS A was activated by the depressurization of the primary coolant system early in the transient. On the other hand HPIS B and accumulator injection system were reserved until the core uncover was calculated to occur after the PCPs tripped in the calculation, in parallel with the EOS[5].
The injection flow rate of both HPIS's were given by the table in the RELAP4/MOD6 input, which describes flow as a function of pump discharge pressure. Tabular data for the L3-6 experiment were taken from the EOS[5].

The accumulator was modeled by control Volume 33, in which the complete phase separation bubble rise model was used. The air was assumed to be present in Volume 33 with the polytropic expansion model (PV^n=const. with n=1.401) in order to simulate the expansion of nitrogen gas in the real system.

3.3 Secondary System Model

The secondary side of the LOFT steam generator was modeled by 3 Volumes, 35, 36 and 37 each representing the downcomer, shroud and steam dome regions, respectively. Volume 35 was homogeneous but the bubble rise model with ALPH=0.6 and V_{BUB} = 1.5 m/s was specified in Volume 36

and complete separation in the steam dome, Volume 37. The vertical slip model was applied to Junctions 42 and 43.

The specified operation of steam generator during the transient was simulated by fill junctions and valve models. The time dependent mass flow rate and fluid enthalpy were specified for the feedwater junction (Junction 40) which simulated both main feedwater and auxiliary feedwater. The main steamline (Junction 44) was closed at early portion of the transient and Junction 46 was continuously discharging with very low steam to simulate the leakage through the steamline control valve. When the secondary pressure reached the opening set point of control valve (7.1MPa = 1020 psia), negative fill junction 47 started to discharge. This model is slightly different from the description in the EOS, in which the control valve operates to control the pressure to between 6.4 and 7.1MPa and this implies the valve action will be cyclic.

The measured data of secondary pressure, however, shows nearly constant pressure rather than the the cyclic behavior for most interval in the early portion of the transient. Thus the negative fill was assumed to be adequate to simulate the control valve, because it usually brings nearly constant pressure around the set point.

Table 3.1 Description of Control Volumes in LOFT System Model

Volume	Description
1, 2, and 3	Nuclear core
4 and 5	Upper plenum
6 and 7	Intact loop hot leg
8 and 13	Steam generator inlet plenum and outlet plenum
9 and 12	Straight sections of steam generator tubes
10 and 11	Curved sections of steam generator tubes
14	steam generator outlet piping to the 16-to-14-in. (0.40-to-0.35-m OD) contraction
15	14-in. (0.35-m OD) piping leading to the tee preceding the coolant pumps
16	Piping from tee to primary coolant pumps
17	Primary coolant pumps
18 and 19	Intact loop cold leg
20	Upper annular region of the vessel inlet region
21	Downcomer region of the reactor vessel
22	Lower plenum
23 and 24	Broken loop cold leg
25, 26, 27, and 28	Broken loop hot leg
29 and 30	Reflood assist bypass piping
31	Pressurizer surge line
32	Pressurizer
33	ECC accumulator
34	ECC injection line
35	Steam generator secondary downcomer
36	Steam generator secondary shroud region
37	Steam generator secondary steam dome

Table 3.2 Description of Heat Slabs in LOFT System Model

Heat Slab No.	Description
1	Nuclear fuels (from bottom to 0.559 M elevation)
2	Nuclear fuels (from 0.559 M to 1.117 M elevation)
3	Nuclear fuels (from 1.117 M to 1.676 M elevation)
4	Steam generator inlet plenum
5, 6, 7 and 8	Steam generator tubes
9	Steam generator outlet plenum
10	Reactor vessel side wall (lower)
11	Reactor vessel side wall (upper)
12	Reactor vessel bottom head wall
13	Lower part of core barrel and flow skirt
14	Upper part of core barrel and flow skirt
15	Upper plenum internals and core barrel
16	Reactor vessel upper head

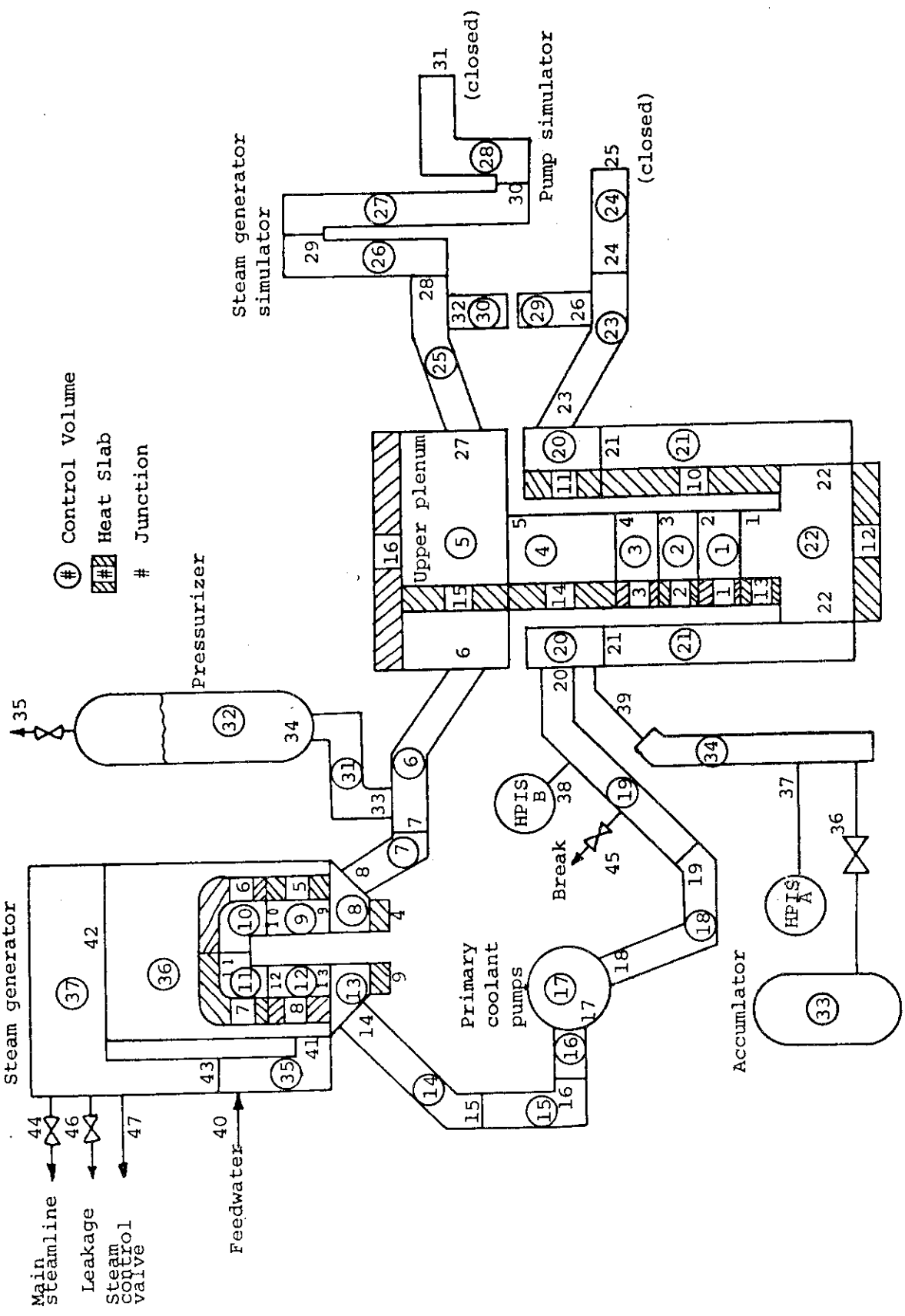

Figure 3.1 LOFT System Model Schematic Diagram

4. Initial Condition

In the small break LOCA, energy balance of the system is important because the energy release rate through break might be comparable order to the heat transfer rate in the steam generator and to the other heat losses. This is in contrast with the case of large break LOCA in which the energy and mass releases by the break flow are dominant in the transient.

Reflecting these situation, simulated initial steady state of the system by a computer code should be strictly balanced about the energy and momentum distributions. If not, the state genearated by the code itself has a tendency to move into another state even without disturbance, and the order of the magnitude of system variable derivatives could be significant in the case of the small break simulation.

Since the automatic steady state initialization capability has not yet implemented into RELAP4/MOD6/U4/J3, we adopt the such capability of the RETRAN code in order to obtain the exact steady state. The input model for RELAP4/MOD6/U4/J3 was at once further converted to the input for the RETRAN code, in order to utilize the steady state initialization capability of RETRAN. After completing the steady state initialization, the pressure and temperature distribution which were given from the RETRAN's steady state was transfered to the RELAP4 model and then the long transient calculation was able to start with sufficiently exact steady state in practice.

The values of major parameters necessary to specify the initial conditions of analysis are listed in Table 4.1. These values were adjusted to the measured data as for as the consistency of the input data is kept.

Table 4.1 Initial Conditions for L3-6 Analysis

Parameter	Used Value	Measured Value
Primary Coolant System		
Mass flow	483.3 kg/s (1065.5 lb/s)	483.3 kg/s
Hot leg pressure	14.87 MPa (2156.7 psia)	14.87 ± 0.14 MPa
Hot leg temperature	577.1 K (579.0 F)	577 ± 1.8 K
Cold leg temperature	557.8 K (544.3 F)	557 ± 1.1 K
Pressurizer		
Steam volume	0.31 m^3 (10.99 ft^3)	0.29 ± 0.06 m^3
Liquid volume	0.65 m^3 (23.11 ft^3)	0.64 ± 0.06 m^3
Liquid temperature	614.5 K (646.48 F)	614.7 ± 1.4 K
Pressure	14.86 MPa (2144.2 psia)	14.90 ± 0.25 MPa
Broken Loop		
Cold leg temperature near reactor vessel	557.6 K (544.0 F)	557 ± 2.6 K
Hot leg temperature near reactor vessel	561.4 K (550.8 F)	561.4 ± 2.6 K
Steam Generator Secondary Side		
Pressure	5.58 MPa (808.9 psia)	5.57 ± 0.06 MPa
Temperature	543.9 K (519.4 F)	542.8 ± 0.8 K
Mass flow	27.8 kg/s (61.29 lb/s)	27.8 ± 0.1 kg/s
Recirulation rate	3.7	———
Liquid inventory	1705 kg (3760 lb)	———
Steam dome volume	3.74 m^3 (131.9 ft^3)	———
Feedwater enthalpy	233.7 kcal/kg (420.6 Btu/lb)	———
Auxiliary feedwater enthalpy	38.9 kcal/kg (70.0 But/lb)	———
Power Level	50.0 MW	50.0 ± 1 MW
Pump Revolution Speed	3159 rpm	———
Accumulator		
Pressure	4.22 MPa (612.3 psia)	———
Temperature	305 K (90 F)	———
Liquid inventory	138.5 kg (6367 lb)	———
HPIS Enthalpy	24.1 kcal/kg (43.3 But/lb)	———

5. Calculational Results and Comparison with the Data

This section gives a general overview of the transient simulation emphasizing the comparison with the data of LOCE L3-6/L8-1.

5.1 General Overview of Transient Simulation

The chronology of the events in the calculation is summarized in Table 5.1 in which the data of LOCE L3-6/L8-1 are also shown.

One of the most important parameter characterizing the LOCE L3-6 is the pressure history as shown in Figure 5.1 and 5.2 for the intact loop hot leg. The transient was initiated by reactor scram at -5.8 s. The main feedwater pump was turned off at this time, and the main steam control valve started to colse and was closed at 6.2 s. These were both simulated by the fill table with linearly decreasing flow rate for feedwater and steam flow.

The break (J45) was opened at time zero. The decrease in pressure prior to the break open was caused by the decrease in power generation due to scram.

Depressurization of the primary system was very rapid for the first few seconds and this initial pressure drop in the calculation was greater than the data and this made the HPIS 'A' initiation at 3.3 s, that is, 0.3 seconds faster than the data. The rate of depressurization was mitigated at about 5 s both in the calculation and the data, because the liquid flow from the pressurizer conpensated partially the loss of primary loop inventory through the break. Pressurizer became empty at 24 s in calculation and at 20.2 s in the data, and about the same time depressurization became faster again until the primary system pressure dropped to saturation pressure. Boiling in the primary system began almost simultaneously in the intact loop between reactor vessel outlet nozzle and the primary coolant pump, at 34,2 s in the calculation. The vapor generated by the flashing was enough to sustain the primary system pressure, and the depressurization rate became very small. The initial boiling in the intact loop hot leg (I.L.H.L) was calculated to occur at 70.4 s, delaying by 36 s from the boiling in the intact loop cold leg (I.L.C.L). On the contrary, the measured data showed that I.L.H.L, I.L.C.L and upper plenum had been saturated at almost same time ($\sim$ 30 s). The difference between calculation and data about the boiling in I.L.C.L made also difference on the time of the end of subcooled break flow, as shown in Table 5.1.

The measured primary system pressure decreased slightly at about 100 s due to considerable amount of steam discharge in the secondary system, caused by the open/close action of steamline control valve. In the calculation, however, the steamline control valve was simulated by the negative fill junction which did not act cycling open/close. Hence the secondary pressure (Figure 5.3) increased to 7.1 MPa (1020 psia), which was opening set-point of the control valve in Experimental Operation Specification (EOS), at 22.8 s and the pressure was kept as the same value until about 350 s. Accordingly the calculated primary system pressure did not show the significant change after the saturation in primary system.

Secondary system pressure, shown in Figure 5.4, decreased gradually and from 700 s the difference appeared between the tendencies of calculated and measured pressure. Calculated secondary pressure varied very closely to the primary pressure after about 400 s. This meant that there was only small temperature difference across the steam generator U-tubes. Primary system pressure dropped below secondary pressure at 1251 s, but the difference between primary and secondary pressure and also temperature were kept very small. On the contrary, measured secondary pressure was kept much higher than primary pressure after 930 s. In the real system, this pressure difference meant that there was significant temperature differece between U-tube primary side and steam generator secondary, at least for saturated portion of heat transfer region. If there was not such large temperature difference for the entire portion of U-tubes, secondary side of heat transfer region in steam generator should filled with subcooled water.

In the former case, the estimated U-tubes heat resistance in the calculation was too small, and in the latter case, the present nodalization for the steam generator secondary was insufficient to simulate the non-equilibrium temperature distribution.

In anyway, steam generator secondary became one of the heat source to the primary system in the later portion of L3-6. In detailed observation, net heat transfer to the primary system had began at about 1060 s in the calculation. It was about 200 s earlier than the pressure reversal, and it was caused because the pressure and temperature in primary coolant system and the heat conducter temperature of the U-tubes were sligthly varying in space.

Depressurization continued with the break serving as the primary

means of heat removal, as shown in the energy release rate through the break, Figure 5.5, which was much greater than the heat transfer rate in the steam generator, shown in the same figure. Figure 5.6 shows the integrated heat transfer rate at steam generator and the decrease of integrated value after 1251 s shows the reverse heat transfer, i.e., from secondary to primary side of steam generator.

At 1856.0 s, the steam generator secondary auxiliary feedwater was manually shut off and at 2371.4 s the primary coolant pumps (PCP) tripped off. These events were simulated by the input data. Primary system pressure was calculated to be 1.86 MPa (270 psia) when PCP tripped off, by 0.41 MPa (60 psia) lower than the actual concition for the PCP trip. Manual termination of HPIS as 2428.2 s was also simulated by the input, and it was the nominal end of LOCE L3-6

Cladding temperature excursion started at 2378 s, first in the middle core then in upper and lower core. It was only seven seconds after the pumps were tripped, while it took twenty-three seconds in the experiment. Calculated PCPs coast down took less than 10 seconds and it was much shorter than the data in which it took about thirty seconds. The difference of the pump coast down rate made calculated core uncovery time earlier than the data along with the difference in the distribution of primary system inventory, which will be stated in the following section. Break isolation at 2460 s and the accumulator actuation and HPIS re-actuation at 2462 s were both simulated by specifying the times by input data. Within a few seconds from restart of ECC water injection, a maximum cladding temperature was attained (2463 s) and then cladding temperatures started to decrease rapidly. After this period, the calculation could be still continued but it took unpractically long computing time. The cause of this trouble was a instability of the calculation due to the strong mixing of cold ECC and superheated steam. This type of instability had been expected by the nature of the code, i.e., the assumption of homogeneous equilibrium state in fluid system. The calculation terminated at 2465 seconds. 2 hours of computing time was spent for the calculation of 3 seconds after ECCS actuation (2462 s), while the total computing time was 3 hours and 56 minutes on FACOM M200 computer system in JAERI.

5.2 Primary System Mass Inventory

The integrated primary coolant system (PCS) mass inventory is shown

in Figure 5.7.

Before about 150 s, calculated decreasing rate of mass inventory was larger than the data, and after that time calculation relatively well predicted the data. Minimum of the PCS inventory was calculated to be 550 kg (1240 ℓb) at the time of break isolation (2460.4 s) while the data showed its minimum to be 650 ± 50 kg (1430 ± 140 ℓ). The comparison of calculated value and with measured break flow is shown in Figure 5.8. It should be noted that "measured" break flow was obtained indirectly by reducing from after kinds of data, and that it contained about 15% uncertainty. Calculated break flow rate laid within the uncertainty limit of the data after about 200 s, but seemed to be larger than the data before 200 s. This made the decrease of PCS inventory faster than the data. Calculated HPIS flow rate agreed with the data in a whole manner, as shown in Figure 5.9. The reason for the stepwise changes of HPIS flow in the data was not clear HPIS flow did not make significant contribution to the change of PCS mass inventory except for the latest portion of LOCE L3-6, because HPIS flow was five to nine times smaller than the break flow for 200 s to 1200 s.

The liquid mass in the reactor vessel (Figure 5.10) was calculated to be 109 kg (240 ℓb) when primary coolant pumps tripped (2371.4 s). There is no available measured data to be compared, but estimating based on the statement in QLR[6] (section 3.1), it was about 300 to 500 kg (650 to 1100 ℓb). Hence reactor vessel mass inventory was underpredicted and its difference between calculation and the data was consistent with the difference in the PCS mass inventory.

5.3 Primary Coolant System Mass Distribution

Fluid density in intact loop hot leg (I.L.H.L), intact loop cold leg (I.L.C.L), broken loop hot leg (B.L.H.L) and broken loop cold leg (B.L.C.L) are shown in Figure 5.11, 5.12, 5.13 and 5.14, respectively. Before approximately 290 s, the data indicated the two-phase fluid in the intact loop was homogeneous (indicated by the similarity in individual density measurement beam in the hot and cold legs) and the calculated densities showed good agreement with the data. After this time and until about 1200 s, when the flow was of high quality, it was observed that the fluid in I.L.H.L was stratified (indicated by the difference between measured density through beam A and C in Figure 5.11). Calculated fluid density, however, was considered the average over the

cross section of the piping because we did not adopt the separated flow model, and the calculated density was consistent with the data. Calculated density for I.L.C.L shown in Figure 5.12 also agreed with the data except for 900 to 1300 s. Measured beam intensities showed that two-phase flow in I.L.C.L was slightly separated at about the same time, although it was almost homogenized by running PCP.

The times of voiding initiations for I.L.H.L and I.L.C.L were almost the same in experiment but were different by 36 s in the calculation. The delay of voiding initiation in I.L.C.L led longer duration of subcooled break flow and then greater mass discharge than the experimental data.

Fluid temperature in the hot leg is usually higher than that in the cold leg, and it was also true in L3-6 [see Ref. (2)]. Local pressure in the cold leg is higher than that in the hot leg when primary coolant pumps run and provide sufficient driving head to the primary coolant. Accordingly, when depressurization due to small break continued and PCPs are running, change into saturated condition of cold leg fluid will delay comparing to the saturation in the hot leg. The delay of cold leg saturation in the calculation simply reflected above situation. Pressure difference across the pump, Figure 5.15 shows the calculated driving head by pump agreed with the data quite well until about 100 s. Hot leg and cold leg temperature, shown in Figure 5.17, also agreed with the data except from 60 s to 150 s when the cold leg temperature became slightly higher than the hot leg temperature in the calculation (due to heat addition by PCP). As long as we consider the usual physical models for the fluid such as incorporated in RELAP4/MOD6, initial voiding in the hot leg should precede the voiding in the cold leg. Hence, it seemed to be necessary to introduce other kinds of models than those in the RELAP4/MOD6 code, in order to explain and to simulate the observed simultaneous voiding initiation in the intact loop.

Fluid properties calculated for the broken loop were different from the data, especially for B.L.C.L and B.L.H.L were earlier than the calculated results, by approximately 100 s in B.L.H.L and by 400 s in B.L.C.L. Fluid temperatures in the broken loop are presented in Figure 5.19 and 5.20. The water inside the broken loop of experimental system was slightly warmed up during the transient but it was not calculated. Changes in the broken loop fluid temperatures before saturation suggested that there were some fluid mixings between pressure vessel and broken

legs. In the calculation, however, the fluid in the broken loop was remaining essentially stagnant until it flashed, hence, there was no temperature rise. The lower temperature in the calculation delayed flashing comparing to the data.

As a problem to be noted, we would describe the followings. The data shows the flashing in the B.L.C.L was earlier than in the B.L.H.L, although the fluid temperature in B.L.C.L never exceeded the temperature in B.L.H.L and the pressure in B.L.C.L were almost the same as that in B.L.H.L. Hence, the difference in the flashing time could not be explained by only static properties of the water. It seemed to be necessary to introduce the discussion about local pressure drop.

Pressure difference in the intact loop across the PCP and steam generator are shown in Figure 5.15 and 5.16, respectively. Calculated differential pressures decreased more rapidly than the data until 200 s. The sudden change in the data at 290 s related to the transition to stratified flow in I.L.H.L As mentioned above, the density calculations in the intact loop showed good agreement with the data before 290 s, hence, PCP model in this analysis seemed to be insufficient to simulate the pump degradation under the two-phase condition.

5.4 Steam Generator Secondary Behavior

Pressure in the steam generator secondary started to increase immediately steamline control valve closed at about 6 s, and reached to control valve opening set point, 7.1 MPa (1020 psia) at 22.8 s in the calculation. Although measured pressure was lower than the opening set point, steamline control value experienced cycling opening at 88.8 s and closing at 99.6 s. In addition, measured pressure was nearly settled to a constant value from approximately 40 s to just before the control valve opened, and also settled to another value after control valve closing as shown in Figure 5.3. This behavior was assumed to be the result of some leakage of steam flow through control valve or the effect of some irregular action of control valve, and were hardly simulated without detailed information about the secondary system. This was the main reason why we had simply adopted the negative fill for the steamline control valve.

Another problem about the secondary system behavior was already shown in Figure 5.4 and briefly stated in Section 5.1. History of calculated secondary system pressure was very close to the primary

coolant system (PCS) pressure (which was mainly controlled by the mass and energy release through the break) after PCS was saturated. This means primary and secondary fluid temperature of heat transfer region in modeled steam generator were very close, because the heat transfer region of steam generator secondary (vol. 36) was always saturated during the transient and, of course, primary side of U-tubes was also saturated after about 40 s.

In contrast with this, measured secondary system pressure decreased more slowly than the PCS pressure. There are two possible causes of these discrepancy. One is the case in which the heat transfer region (bundle region) in the steam generator secondary side was filled with saturated or almost saturated water but the heat transfer rate from secondary side to primary side of U-tubes significantly decrease due to the high quality two-phase flow in the primary side, i.e., thermal resistance became larger than in the calculation. Another case is also possible, in which the U-tube bundle region of secondary side (at least partially) filled with subcooled water with almost equal temperature to the primary coolant, so that no significant heat transfer took place. In this case a strong unequilibrium in space is expected in steam generator secondary liquid because the liquid near the steam dome must be always saturated. It is difficult to identify which case really occured during the LOCE L3-6 because there was limited information about the secondary system behavior. If the former case was true, calculated heat transfer rate at the steam generator U-tubes was overestimated for the reversal heat transfer. If the later was true, main reason for the discrepancy between data and calculation should be due to the insufficient noding model for the steam generator.

Figure 5.18 presents a comparison between calculated and measured liquid levels in steam generator downcomer. The small but very rapid increase of measured liquid level at about 90 s was due to the level swelling followed by the steamline control valve opening, and could not be simulated in the present calculation because we adopted the negative fill model for the steamline control valve so that complex action of control valve did not occur. Except for this rapid change, the measured liquid level were continuously increasing after about 100 s according to the auxiliary feedwater injection. Calculated liquid level, however, decreased more after auxiliary feedwater started (73.4 s) and reached its minimum at approximately 400 s, then increased until auxiliary

feedwater stopped. As mentioned early in this section, heat transfer region of steam generator secondary was modeled by single volume (vol. 36) and it was always saturated in the transient. Hence, the cold water from the downcomer easily caused condensation of steam in the heat transfer region. Steam condensation induced the void collapsing and the decreasing of water heat in the heat transfer region, then it induced the decrease of liquid level in the downcomer. In the real system, however, steam condensation might take place in the limited region (did not occur at the whole space of the heat transfer region), hence the induced level drop should be smaller than the calculation.

The prediction of steam generator liquid level was not playing an important role in the analysis of LOCE L3-6. However, it should be noted that steam generator liquid level should be properly predicted in the case of many operational and abnormal transients in PWR plans, because it might affect the control and protection system behaviors.

5.5 Cladding Temperatures

Fuel cladding temperatures of the three heat slabs in the modeled core are shown in Figure 5.22. After the reactor scram, rapid decreases of cladding temperatures occured, and until approximately 1460 s, cladding temperatures were varying with slightly higher value than the saturation temperature because the saturated nucleate boiling continued in this interval. According to the increase of void fraction in the core (as shown in mid-core quality in Figure 5.23), critical heat flux decreased and DNB was calculated to occur at 1460 s in the midcore, immediately followed by DNB's in upper and lower core portions. Then heat transfer regime shown in Figure 5.4 changed into "high flow film boiling (Mode6 in RELPA4/MOD6)" and wall superheat increased due to the reduction of heat transfer coefficient. When PCP stopped at 2371.4 s, rod temperature excursion began with only 7 s delay, in contrast with the data in which temperature excursion started at 2394.6 s (Figure 5.25). The main cause of the difference on the starting time of temperature excursion was thought to be higher predicted core quality due to more rapid pump coast down than the data. Although there were no direct measurement of the fluid condition in the core, it was able to suppose that the quality and also void fraction in the core were calculated to be higher than the data for the later portion of the transient and this caused the early DNB at 1470 s in the modeled core.

As mentioned earlier, mass inventory in the reactor vessel was predicted smaller than the data, and in addition, most of the water in the reactor vessel was accumulated in the upper plenum in the calculation. Both of these contributed to making the core fluid condition more severe than the data. Increasing rate of fuel cladding temperature was measured to approximately 2.5 K/s (5.4 F/s) at the maximum power elevation of 0.74 m (26 inches) in the center fuel bundle.

The calculated temperatures corresponded to three core section heat slabs so that they represented the temperatures of three representive elevations of a fuel rod which had core-wise averaged power generation rate. The temperature calculated for the core center heat slab [No. 2, elevation from 0.559 m (22 inches) to 1.118 m (44 inches)] was shown in Figure 5.25 which had the increasing rate of 1.4 K/s (2.5 F/s). In the same figure also shown was measured temperature at the elevation of 0.813 m (32 inches) of central fuel assembly (TE-5H6-032) which had the increasing rate of 1.9 K/s (3.4 F/s). Power generation rates corresponded to those fuel rods and elevations are different by the factor 1.4, which is very close to the ratio of heat-up rates of 1.9 K/s and 1.4 K/s (power generation rate for the rod No. 5H6 was not found but measured linear heat rate for the rod No. 5H8 were listed in reference (2), which we used for above evaluation). In Figure 5.25, the data for the highest power elevation (26 inches) in the peripheral bundle (TE-4F9-026) was also shown, because its power generation rate was assumed to be nearly the same as one for modeled heat slab No. 2 and it showed almost the same heat-up rate as the calculated value.

According to the above discussions, core heat transfer during the fuel temperature excursion were correctly simulated by the model of convective heat transfer to superheated steam. Temperature increasing rates in the calculation and the data, all of them were slightly smaller than the adiabatic heat-up rate, were different each other only because of the different power generation rates.

Rod quenching occured just after the initiation of accumulator at 2462.2 s. The flow of subcooled ECC (injected to downcomer in the modeled system) caused the condensation of steam in the downcomer and lower plenum. The liquid started to flow from upper plenum to these low pressure region through the core, hence the rewetting of the rods were induced.

Table 5.1 Calculated Sequence of Events for ISP-No.11 (LOFT L3-6)

EVENT	TIME (S) Calculation	Data
Start of Calculation	-5.8	———
Reactor scrammed	5.8*	-5.8 + 0.2 - 0.0
LOCE initiated	0.0*	←
HPIS 'A' injection initiated	3.3	3.6 + 0.0 - 0.2
Steamline control valve closed	6.2	5.6 + 0.0 - 0.2
Steamline control valve opended at 7.1 MPa	22.8	
Pressurizer emptied	23.0	20.2 + 0.0 - 0.2
Initial voiding in intact loop hot leg	34.2	29.4 ± 5.0
Upper plenum fluid saturated	38.1	28.5 ± 0.2
Initial voiding in intact loop cold leg	70.4	31.4 ± 5.0
End of subcooled break flow	71.2	44.2 ± 0.2
Initiation of reverse heat transfer in SG (from 2ndary to 1ry system)	1060	———
Primary system pressure became less than secondary system pressure	1251	930 ± 30.0
Primary coolant pumps tripped off	2371.4*	←
Cladding temperature excursion started	2378	2394.6 ± 0.2
Break isolated	2460.4*	←
Accumulator initiation	2462.2*	←
Maximum cladding temperature	2463	2465.8 ± 0.2
End of calculation	2465	———

*) specified by input data, not the calculated results.

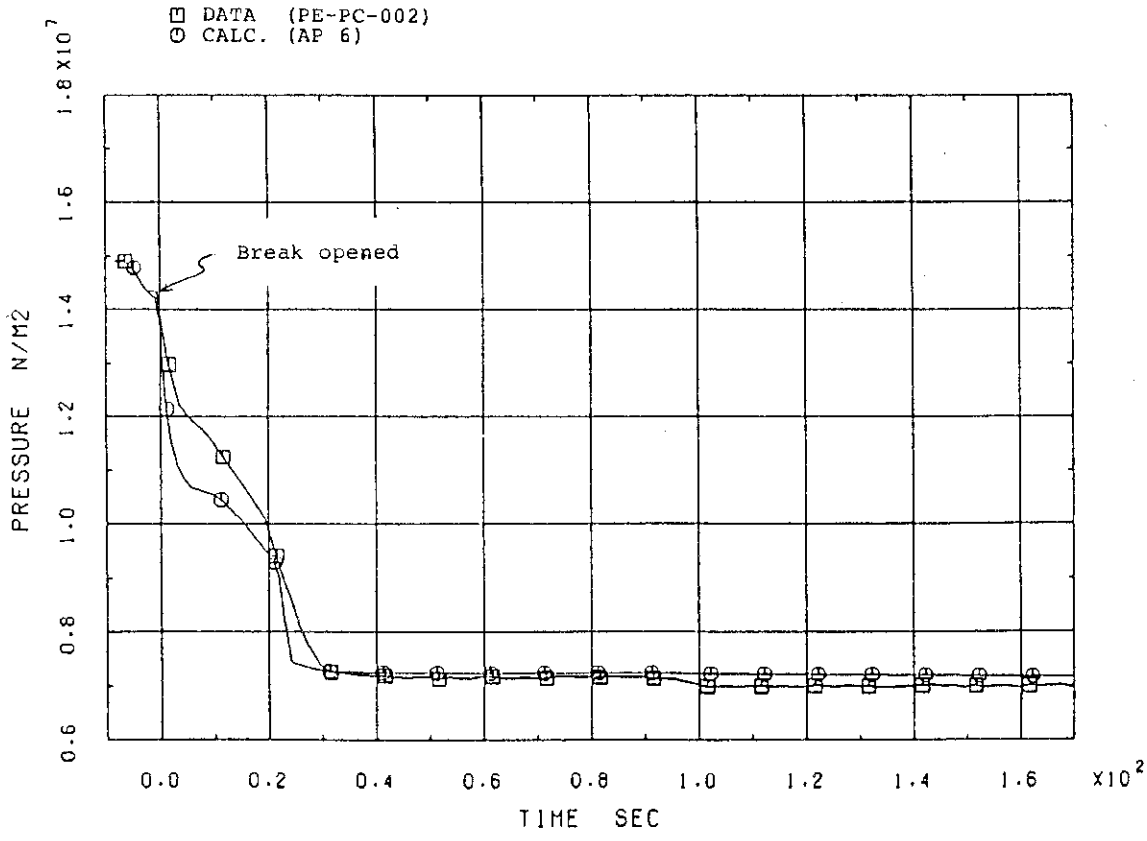

Figure 5.1 Primary Coolant System Pressure at Intact Loop Hot Leg (short range)

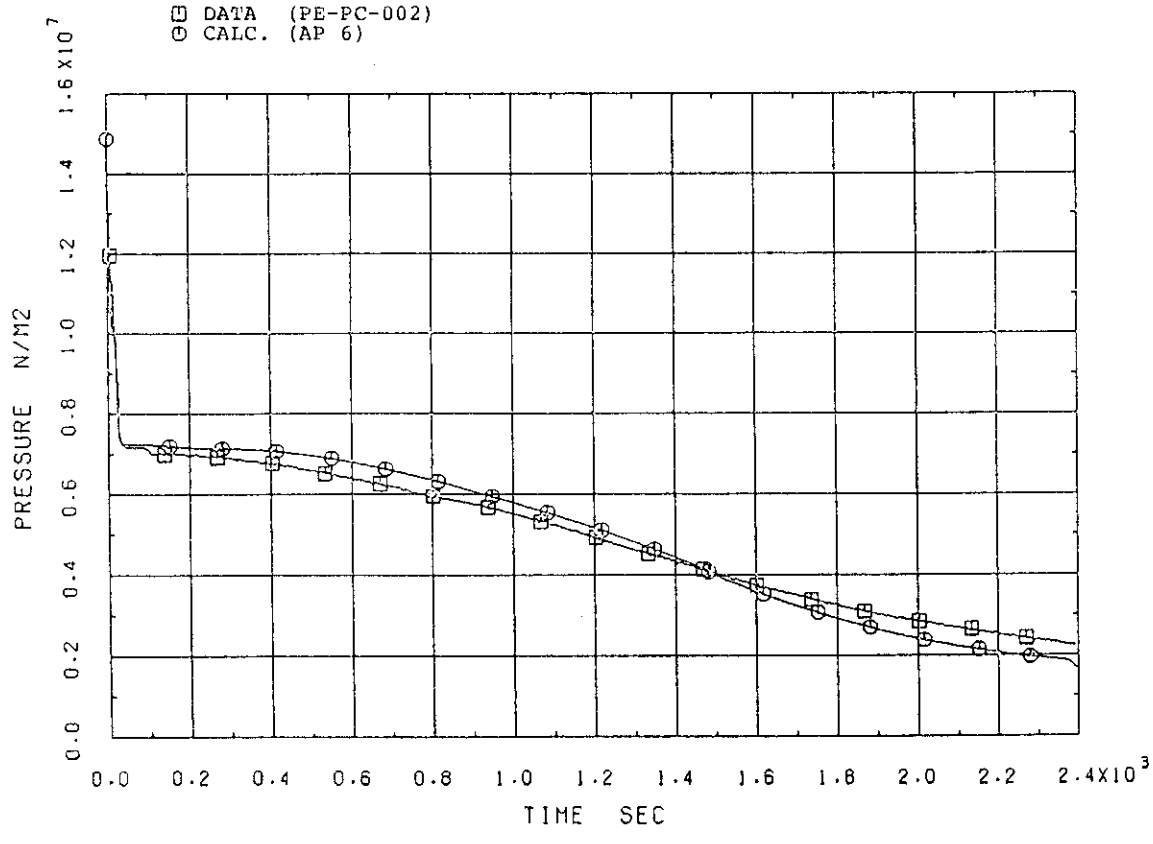

Figure 5.2 Primary Coolant System Pressure at Intact Loop Hot Leg (long range)

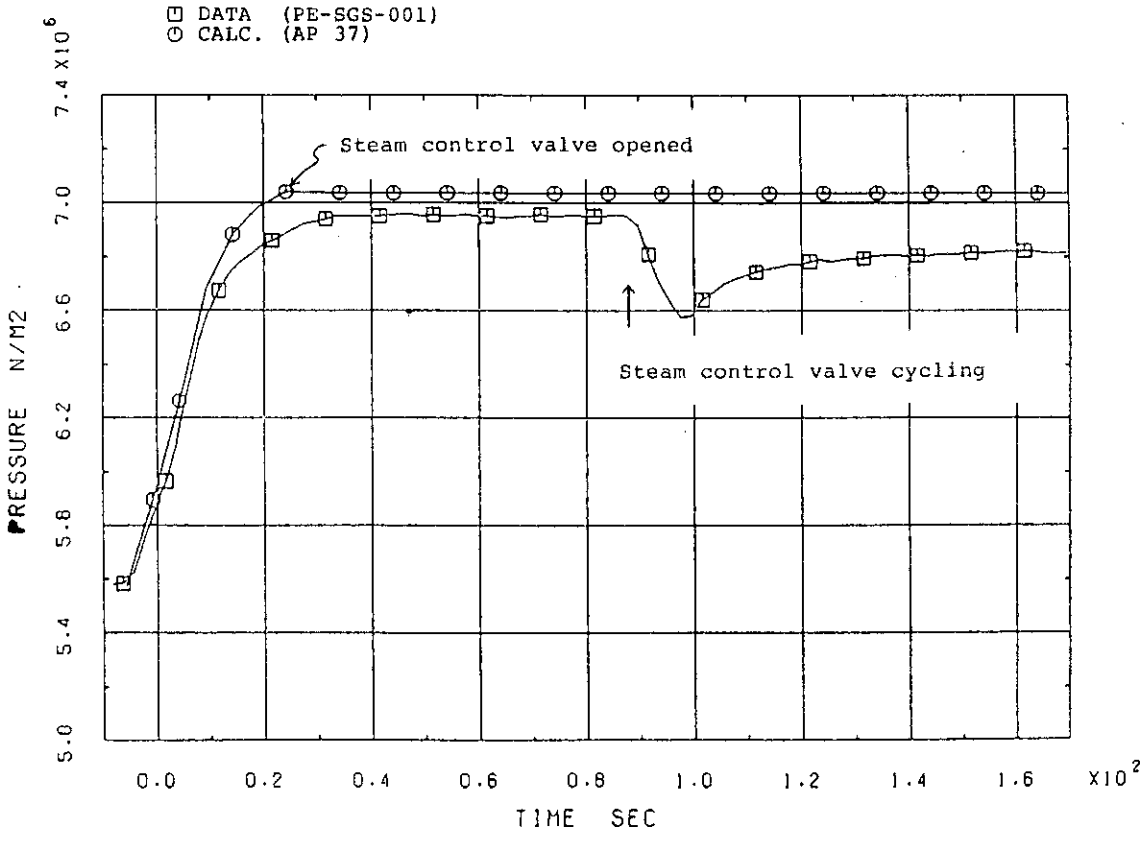

Figure 5.3 Steam Generator Secondary Pressure (short range)

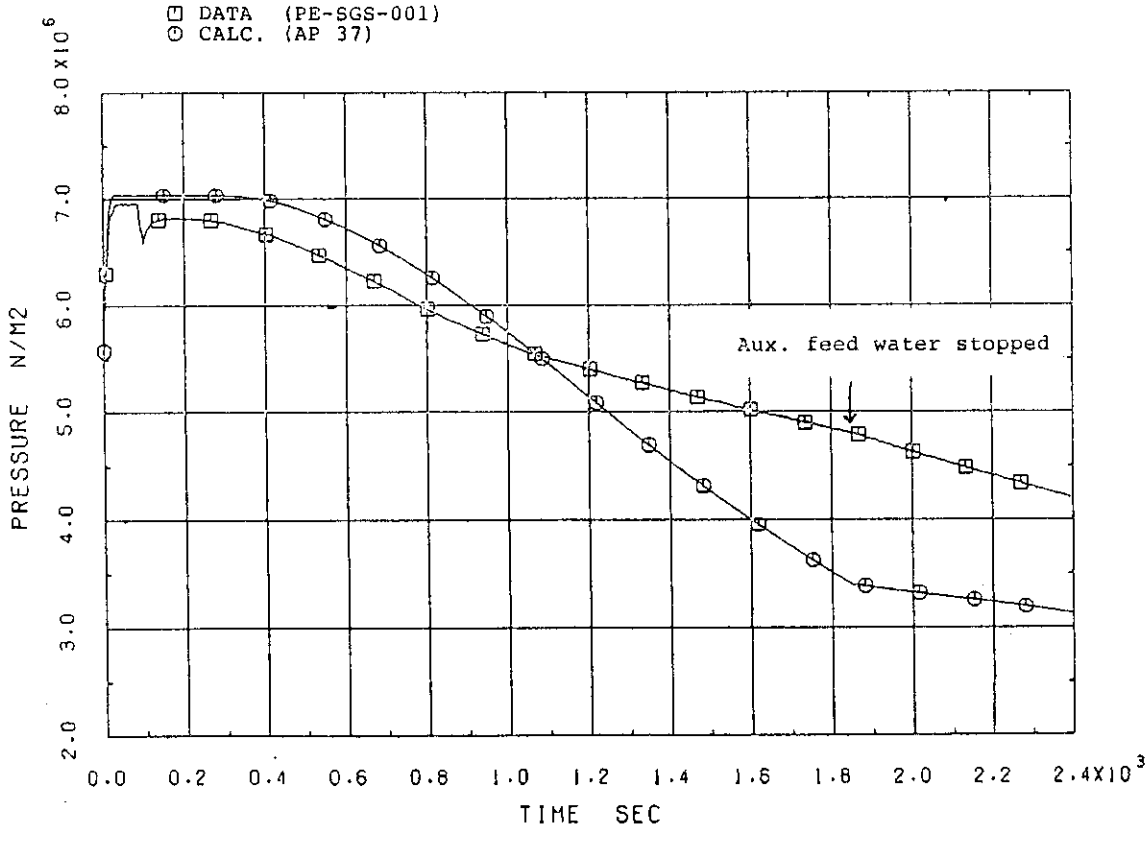

Figure 5.4 Steam Generator Secondary Pressure (long range)

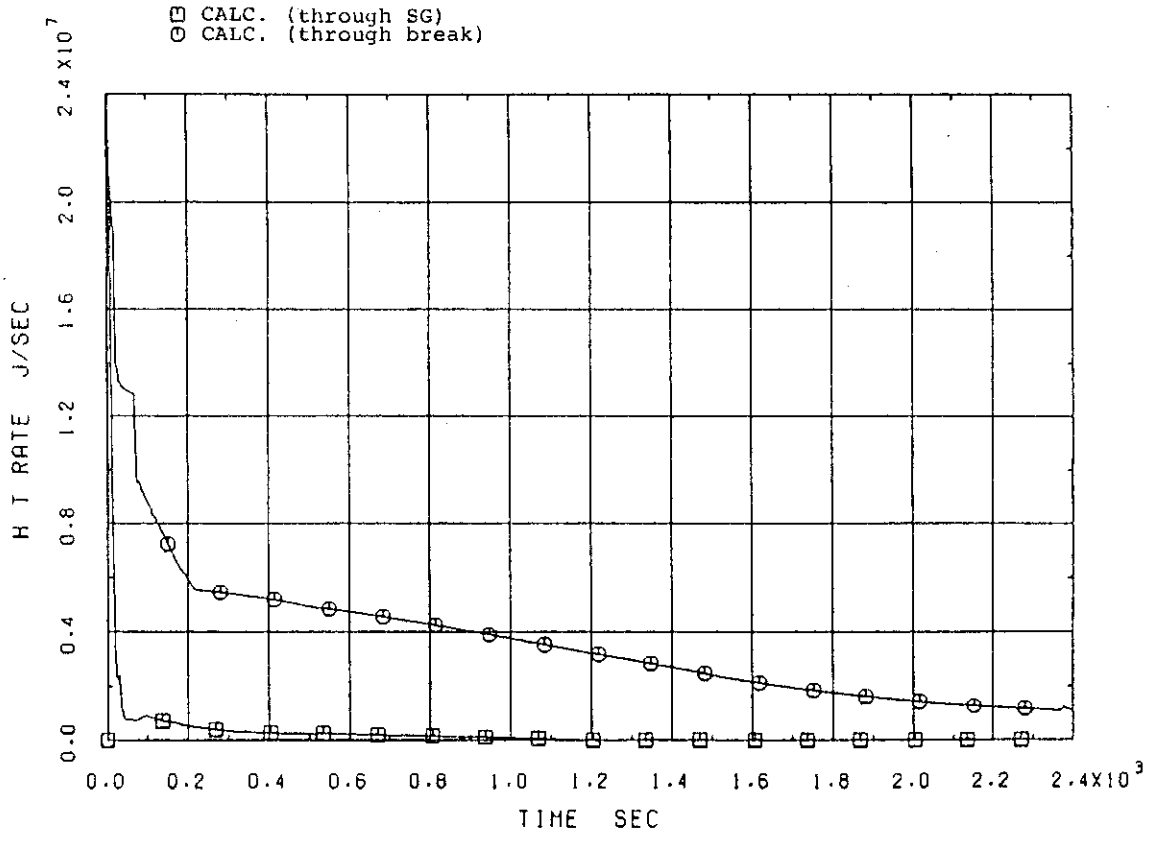

Figure 5.5 Heat Removal Rate from Primary Coolant System through Steam Generator and through Break

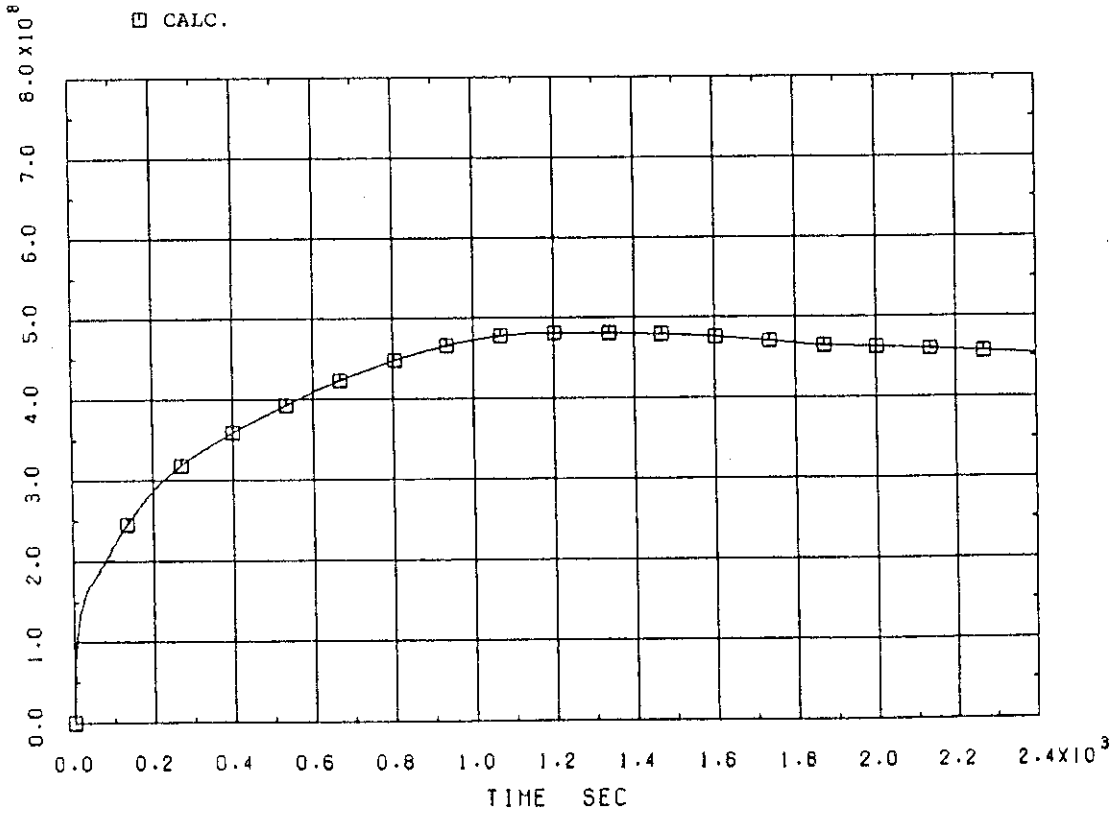

Figure 5.6 Integrated Heat Removal Rate through Steam Genarator

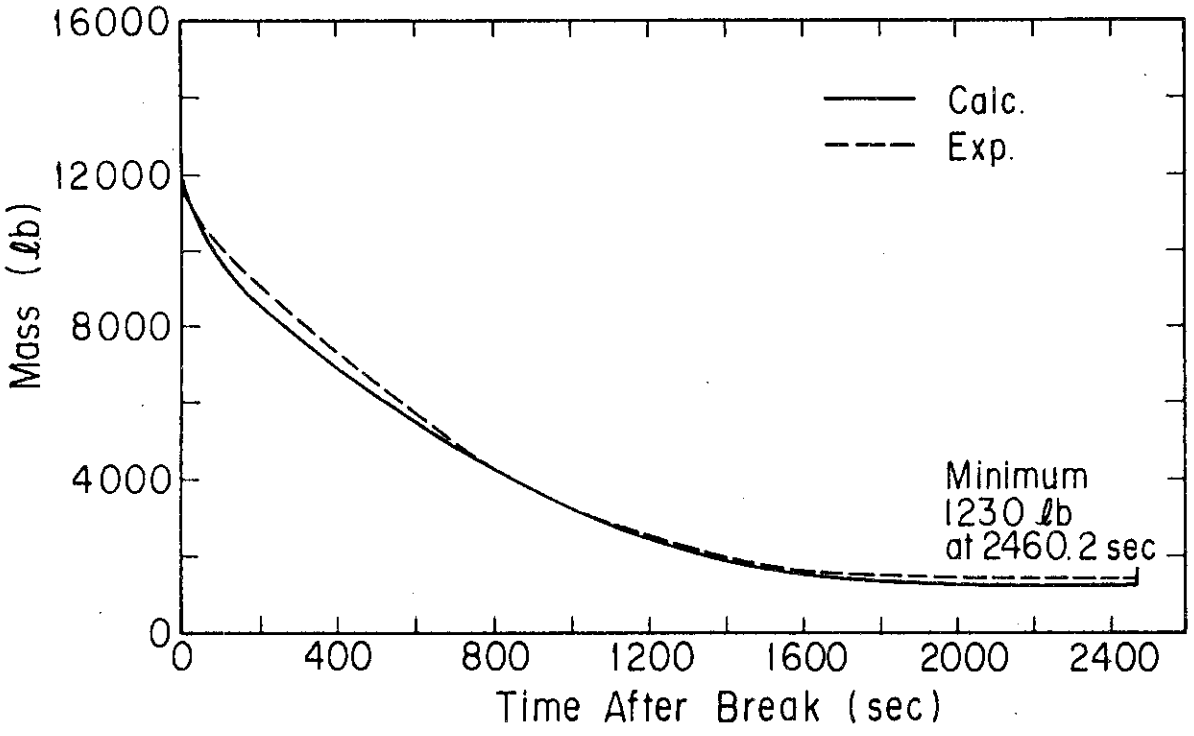

Figure 5.7 Total Coolant Mass in Primary Coolant System

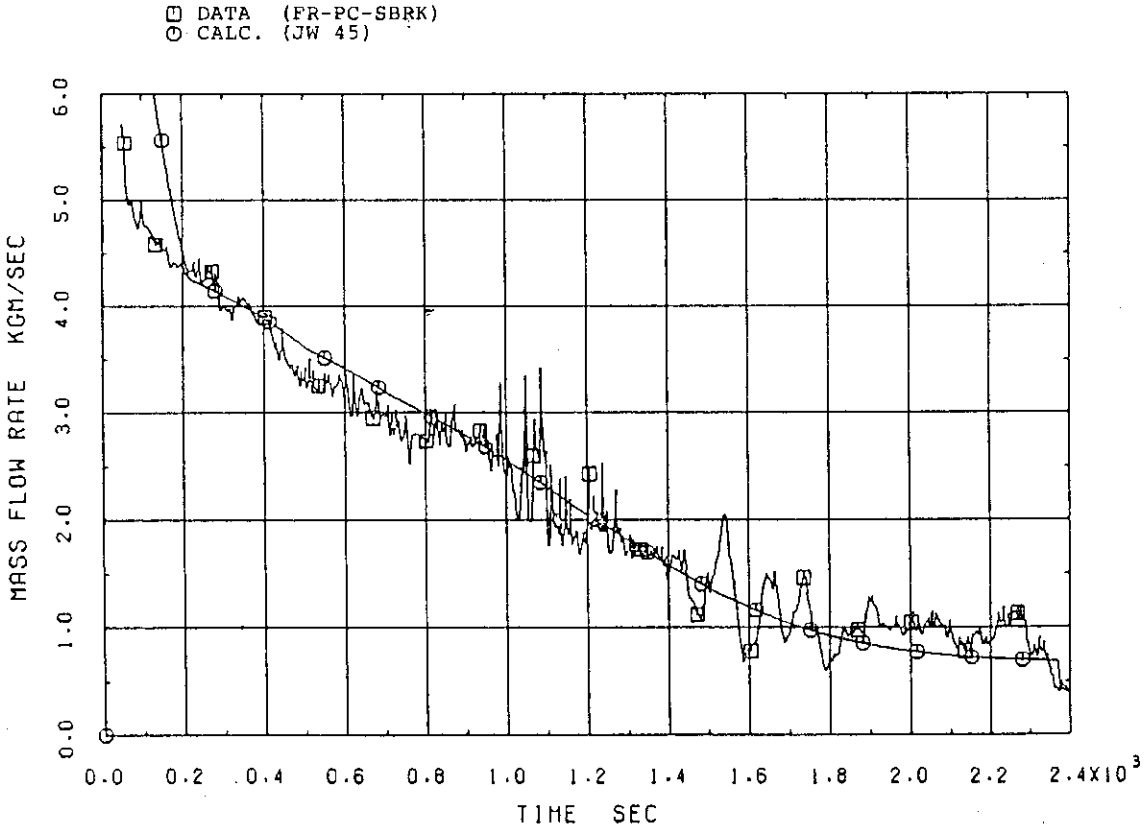

Figure 5.8 Mass Flow Rate through Break

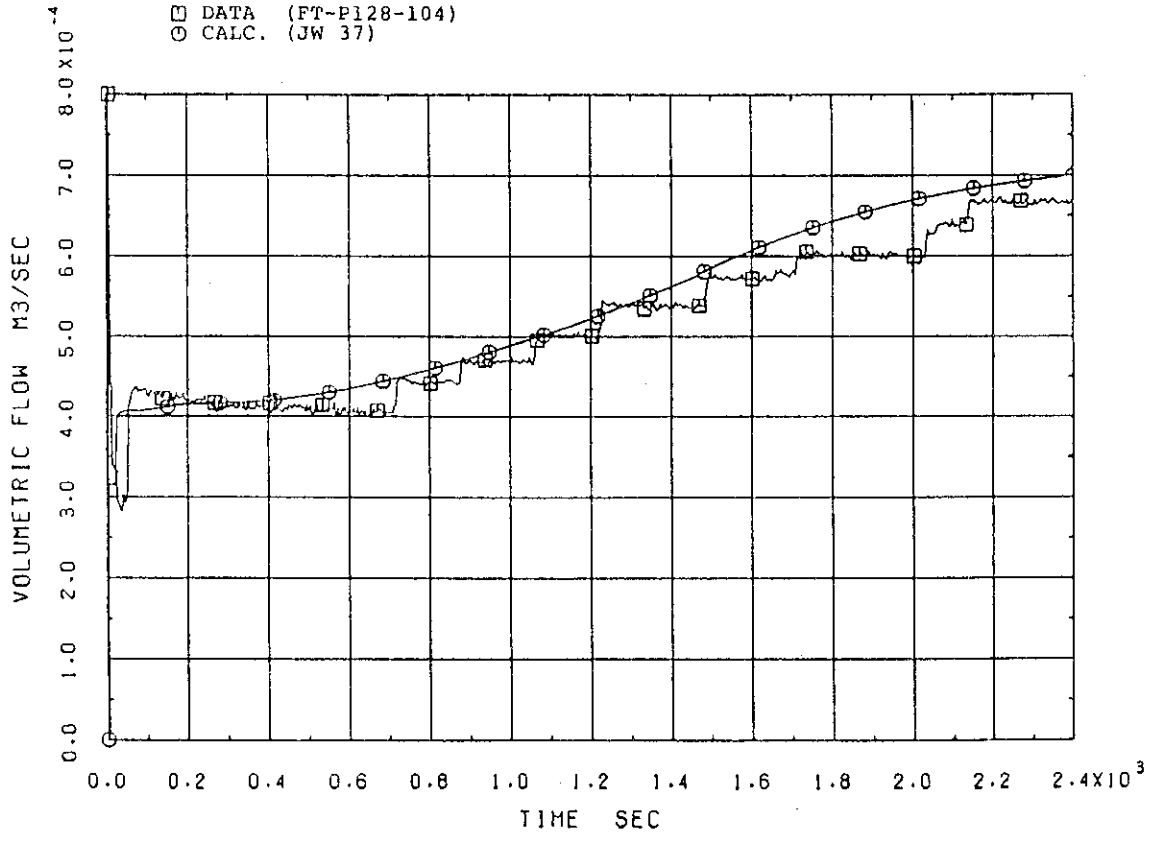

Figure 5.9 Volumetric Flow Rate of HPIS A

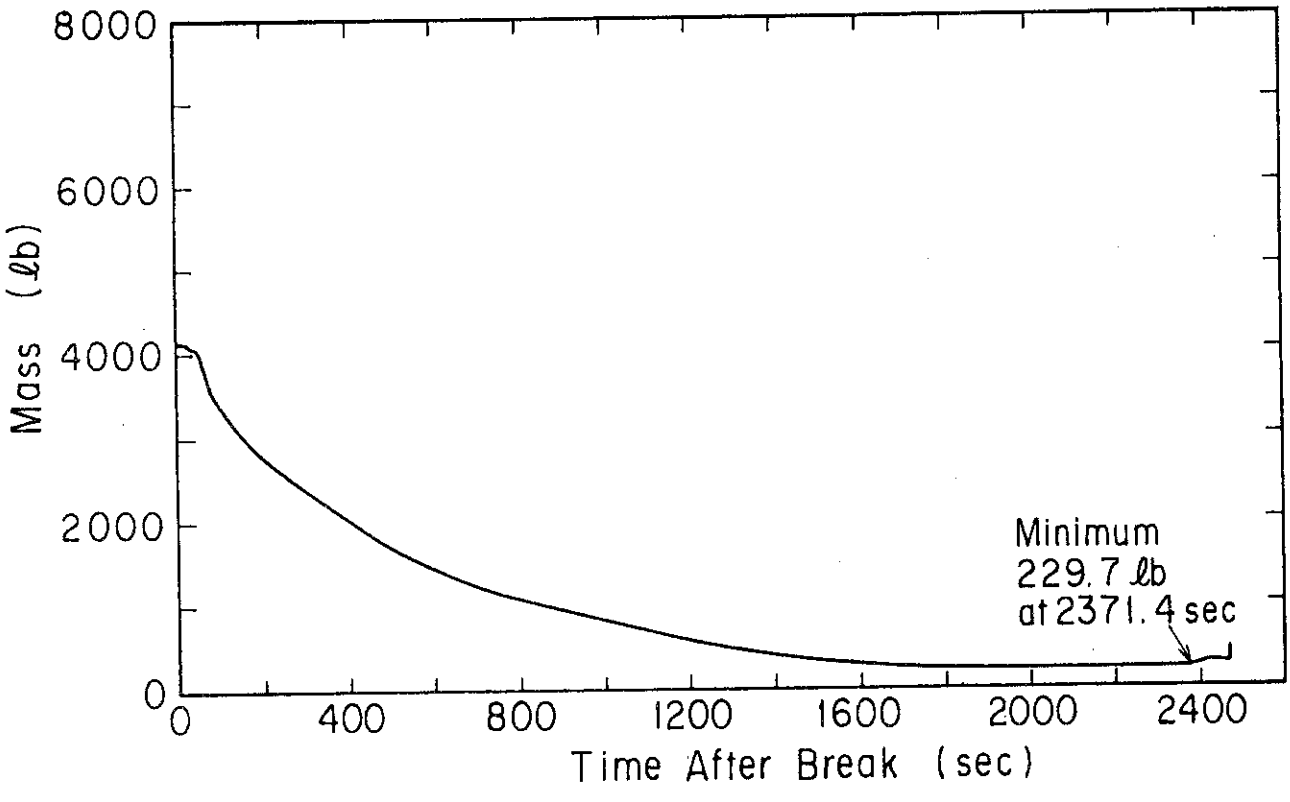

Figure 5.10 Total Coolant Mass in Reactor Vessel

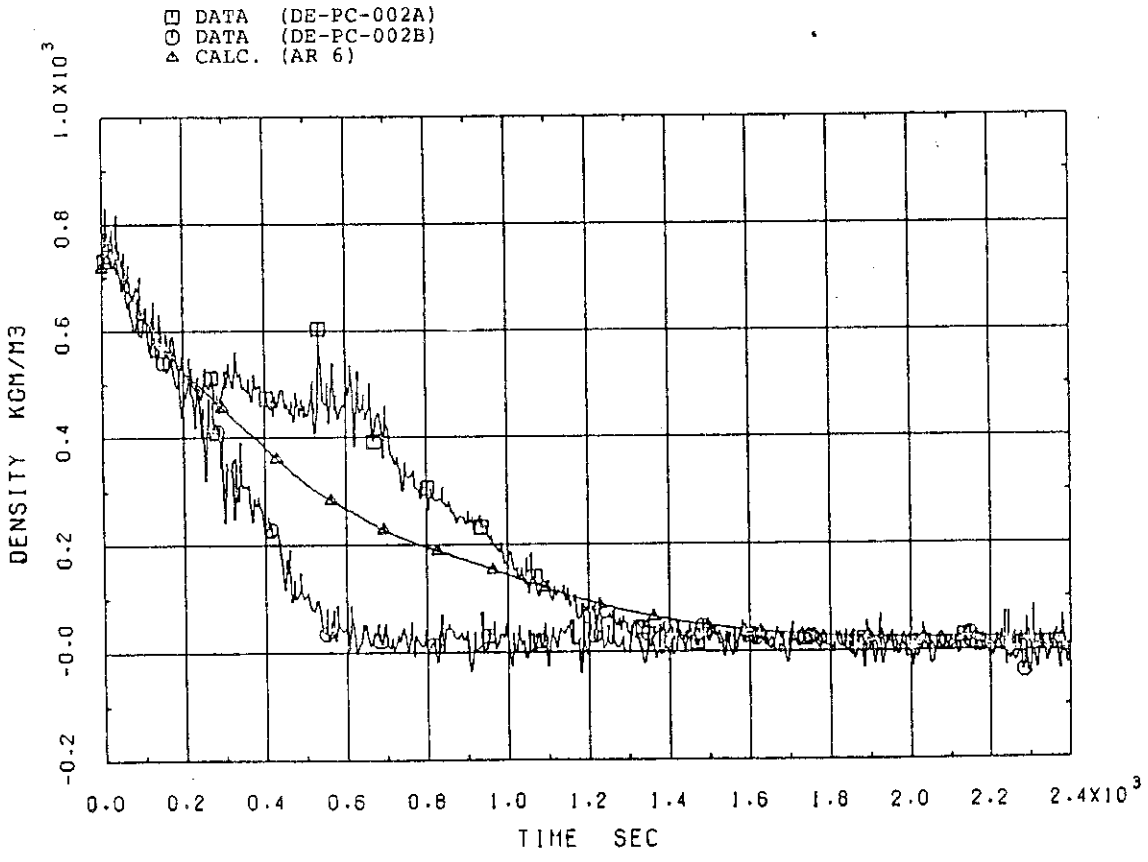

Figure 5.11 Fluid Densities in Intact Loop Hot Leg

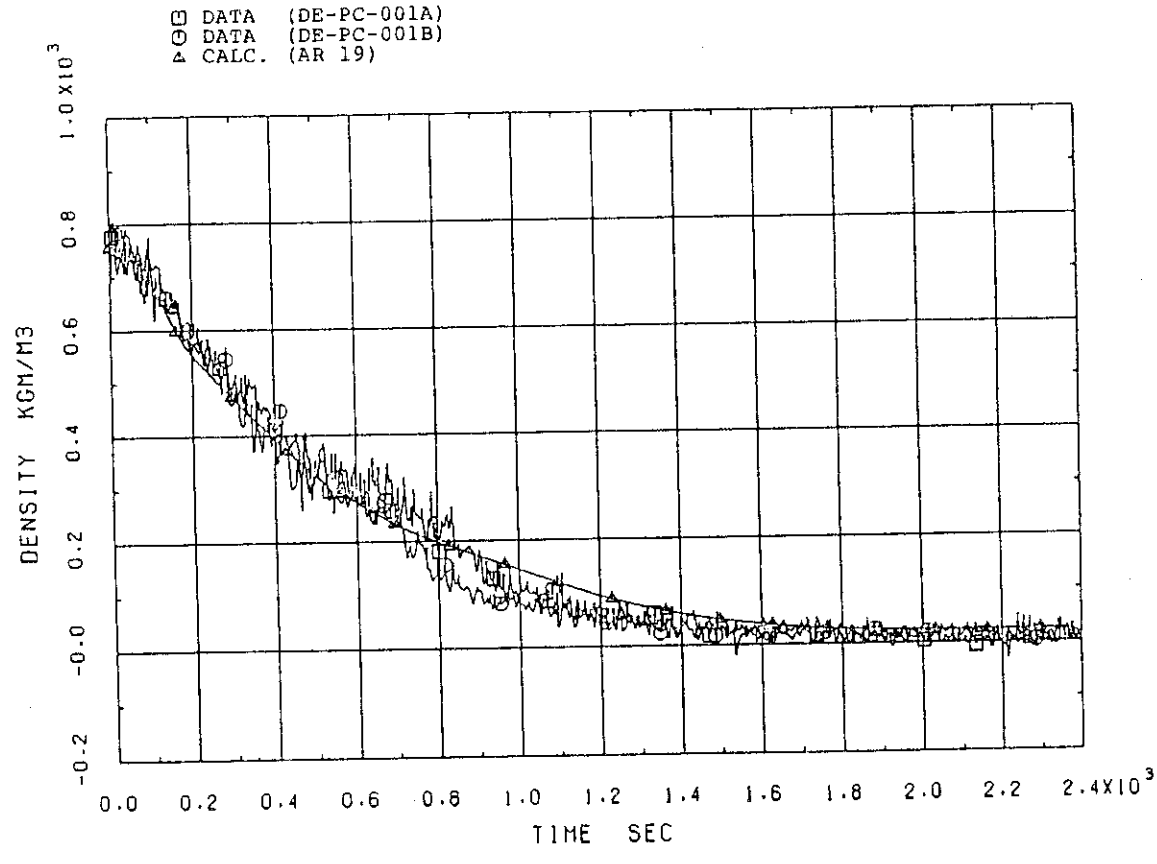

Figure 5.12 Fluid Densities in Intact Loop Cold Leg

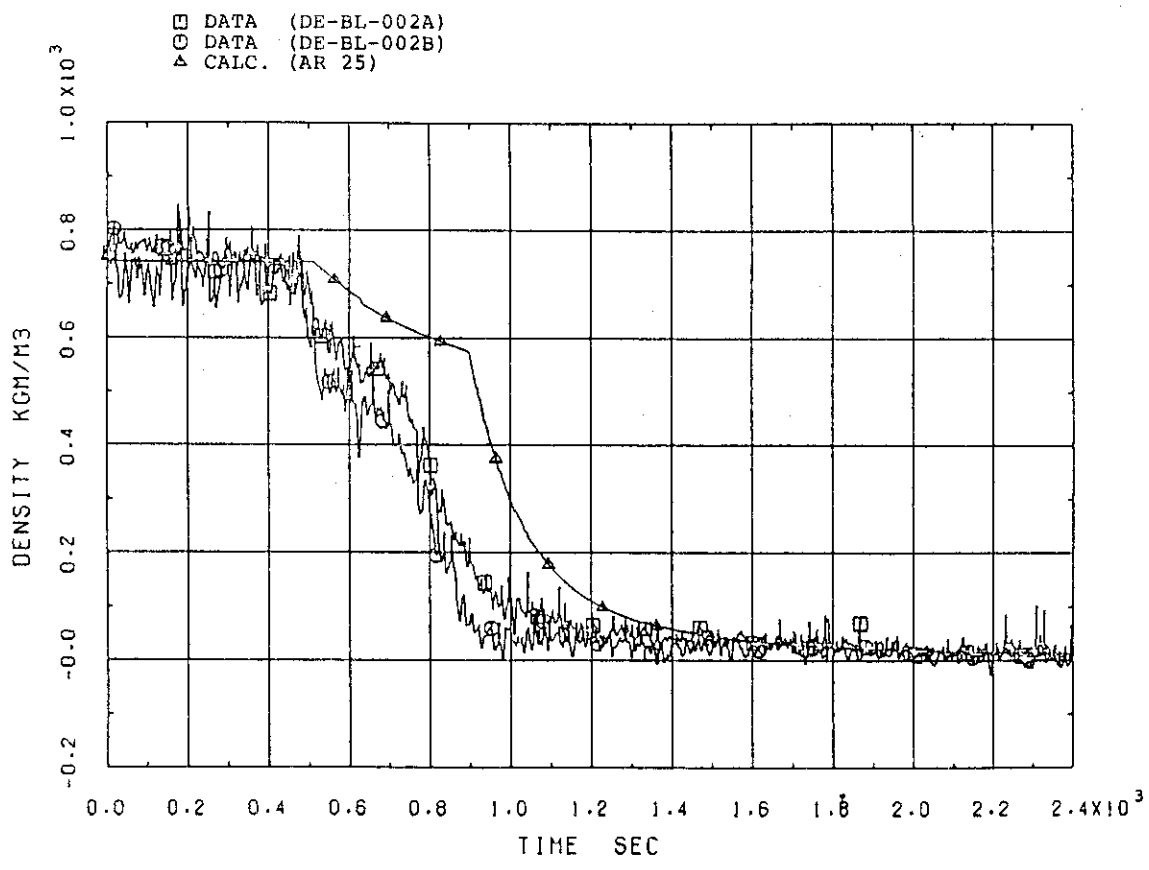

Figure 5.13 Fluid Densities in Broken Loop Hot Leg

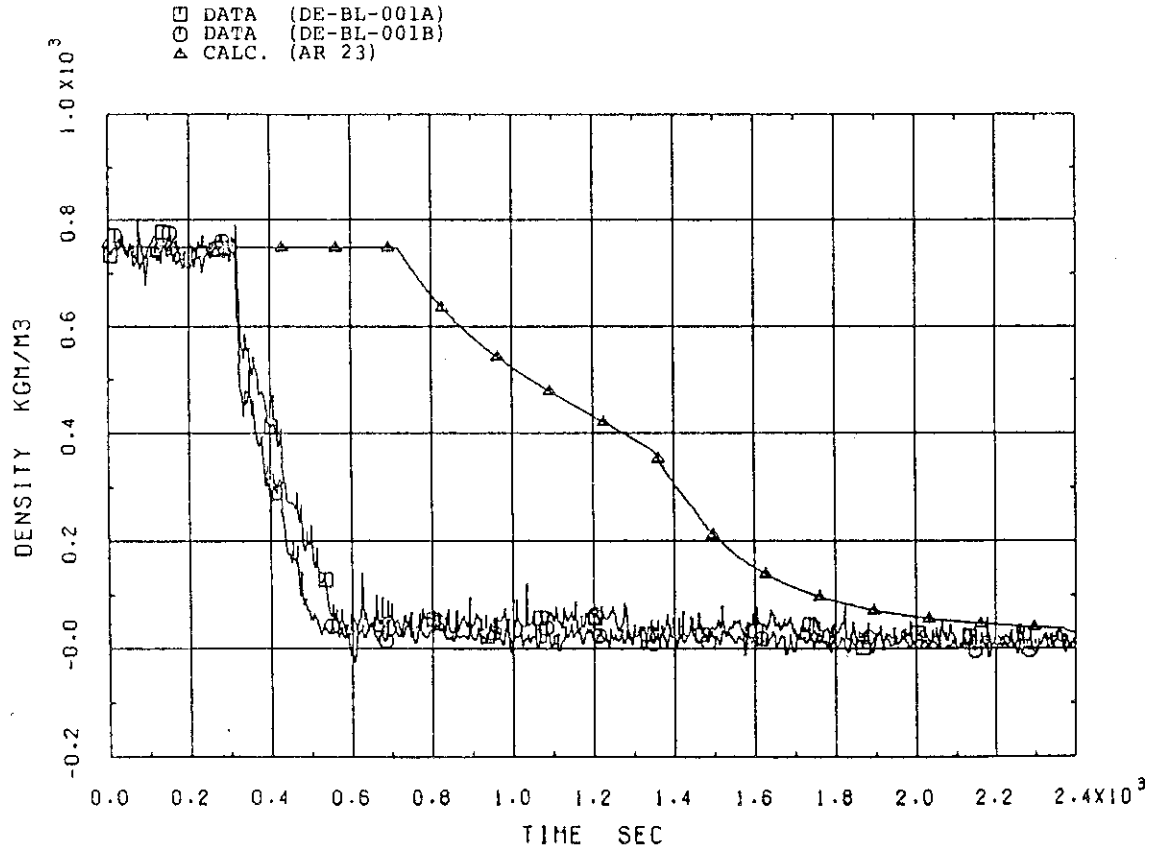

Figure 5.14 Fluid Densities in Broken Loop Cold Leg

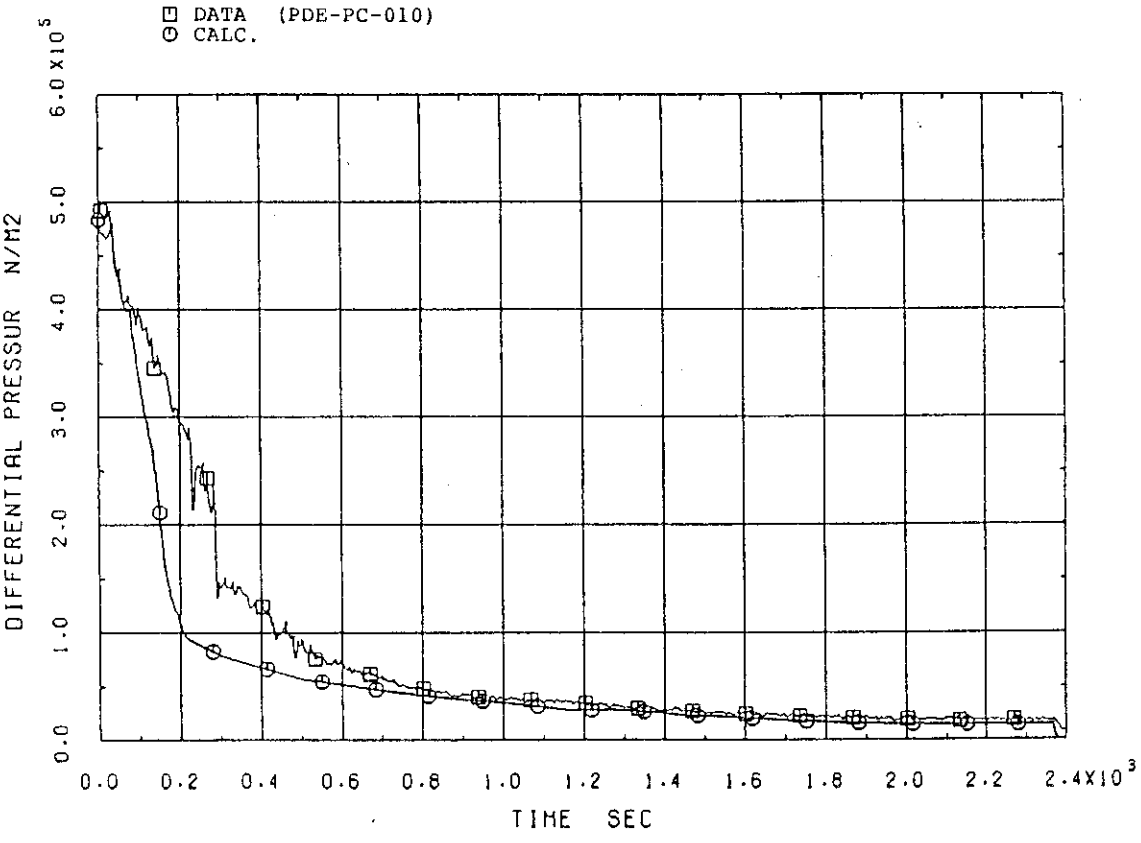

Figure 5.15 Differential Pressure across Pump

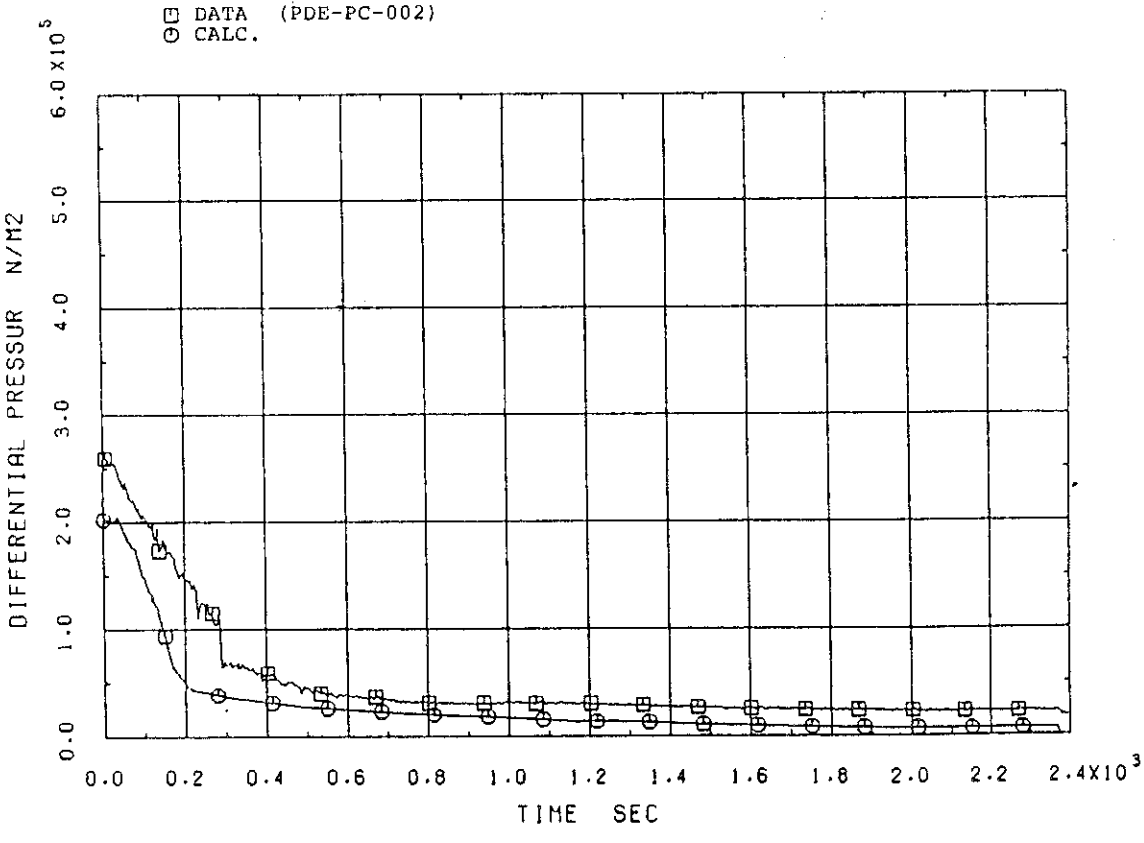

Figure 5.16 Differantial Pressure across Steam Generator

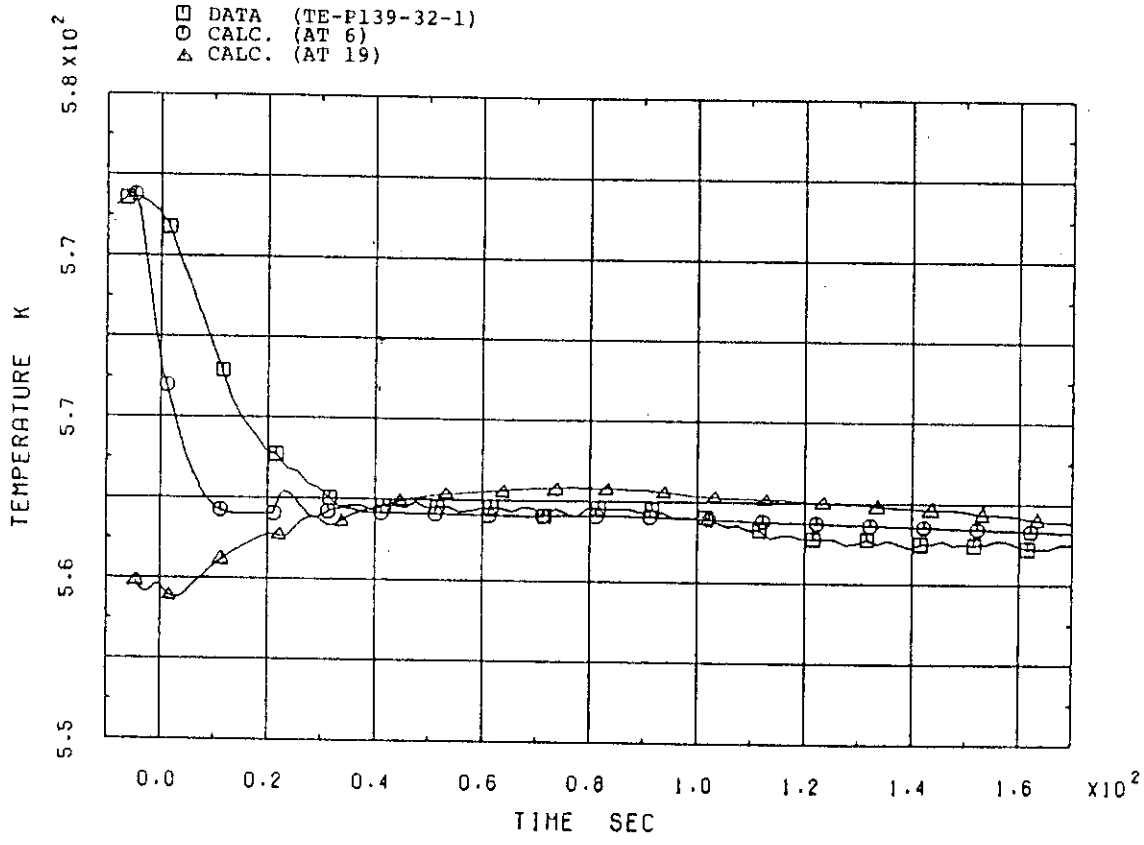

Figure 5.17 Intact loop Fluid Temperature at Hot Leg and Cold Leg (short range)

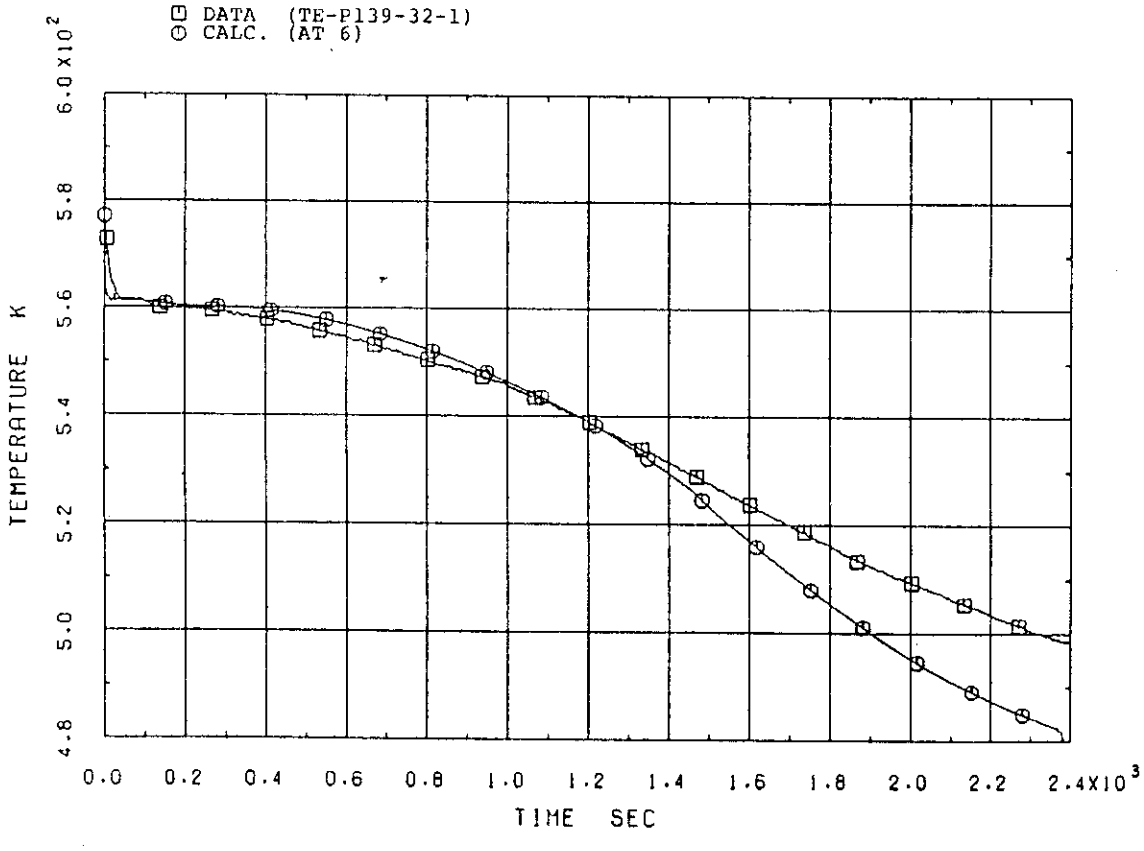

Figure 5.18 Intact Loop Fluid Temperature at Hot Leg and Cold Leg (long range)

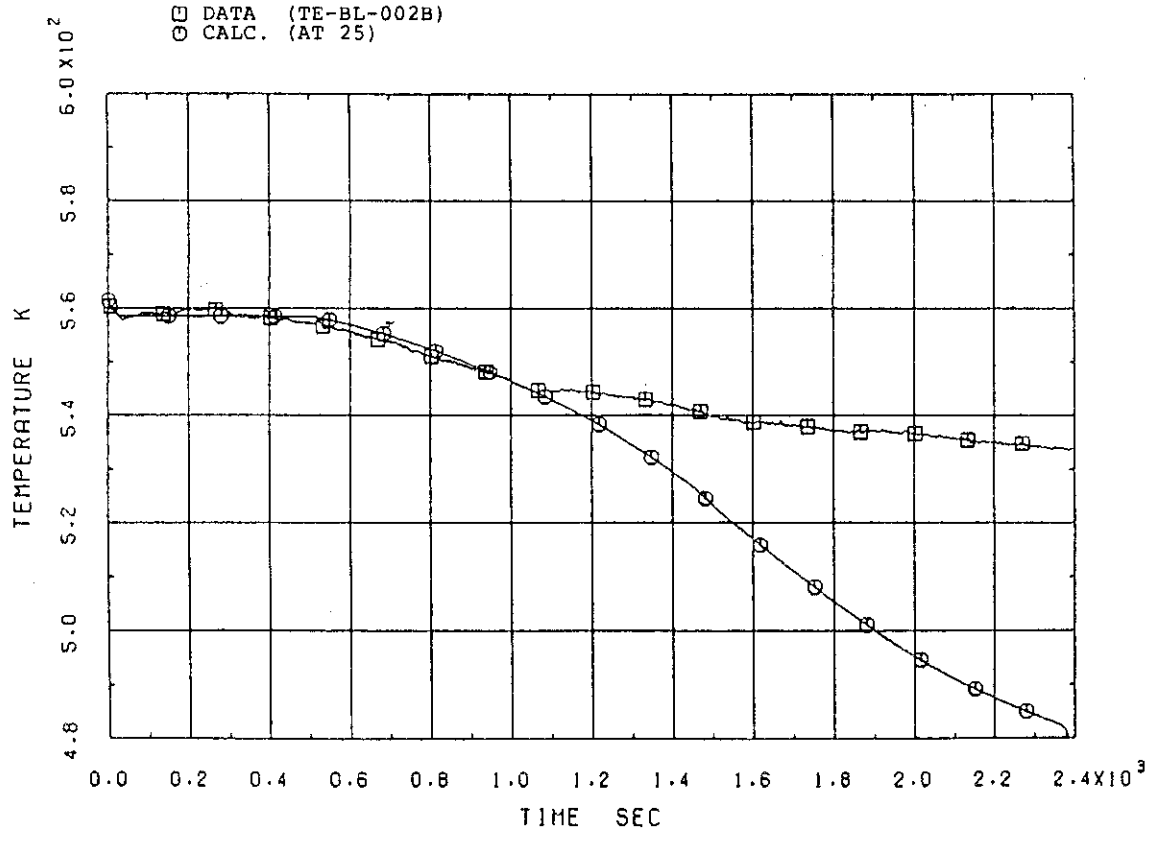

Figure 5.19 Fluid Temperature in Broken Loop Cold Leg

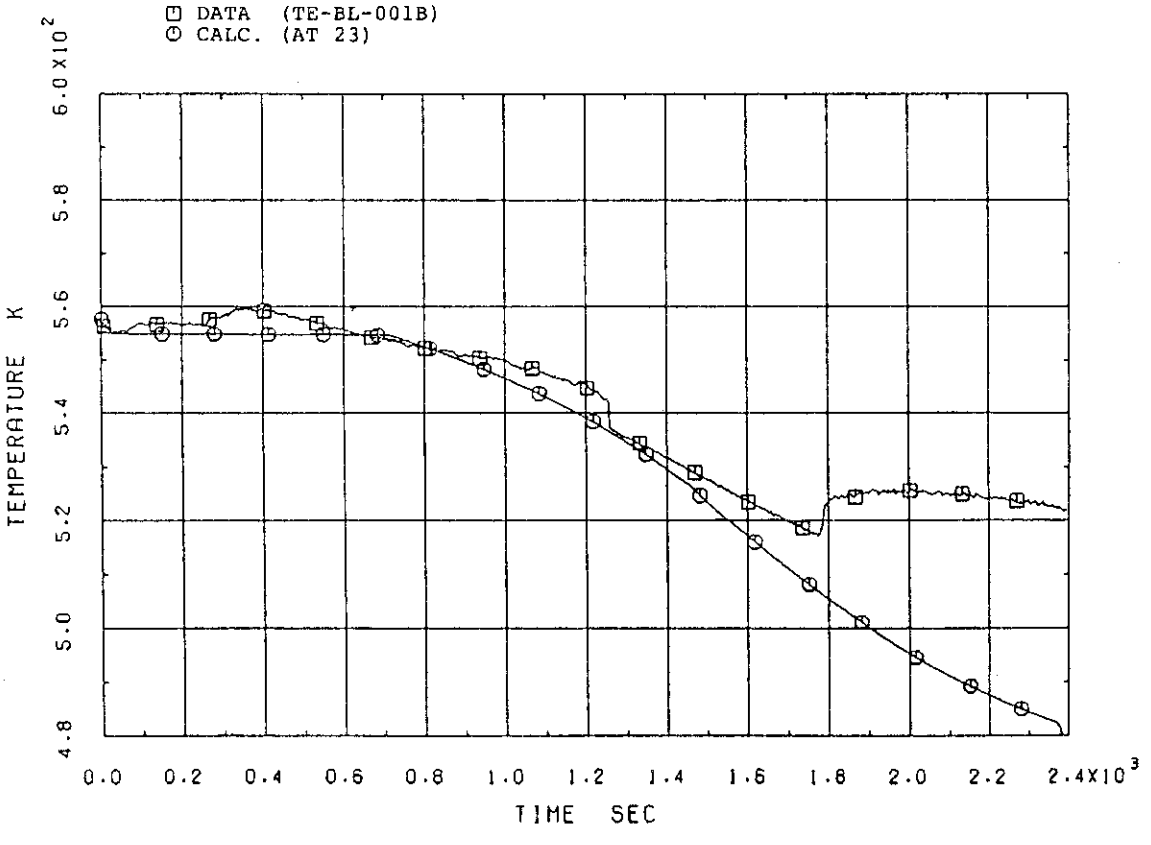

Figure 5.20 Fluid Temperature in Broken Loop Hot Leg

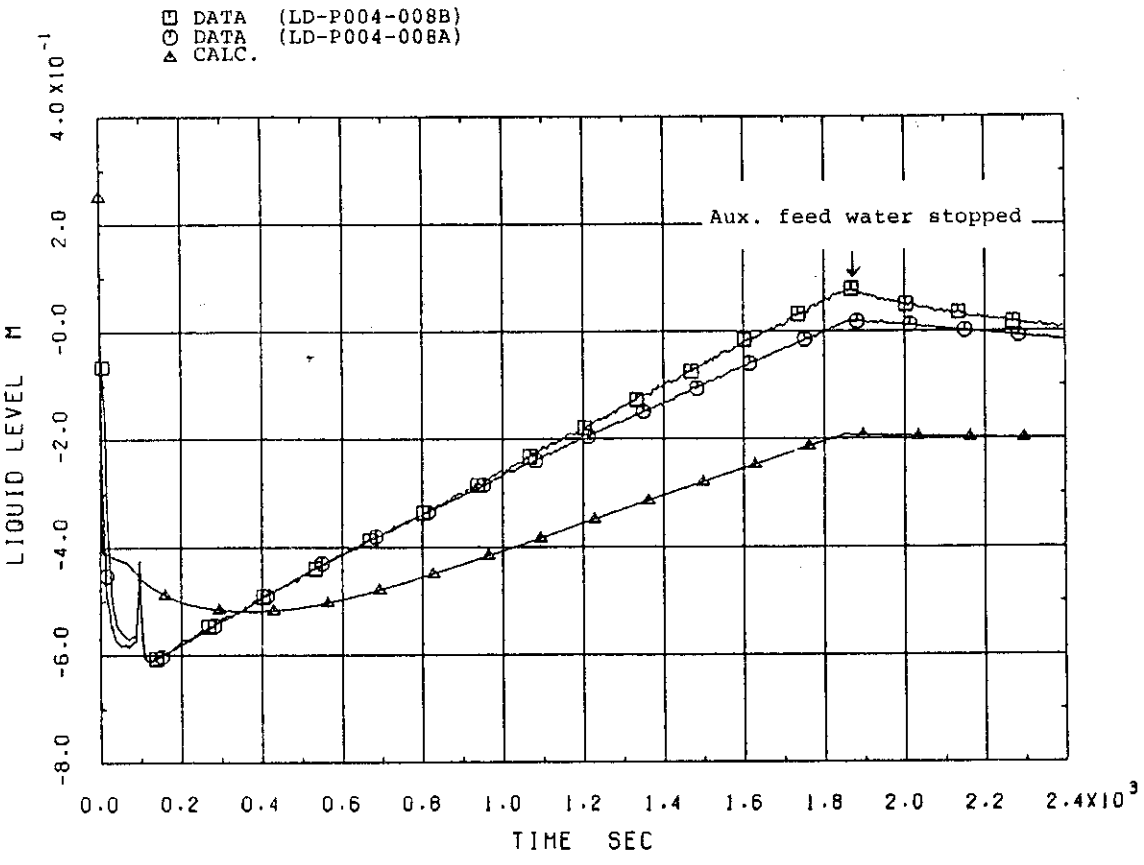

Figure 5.21 Steam Generator Secondary Liquid Level

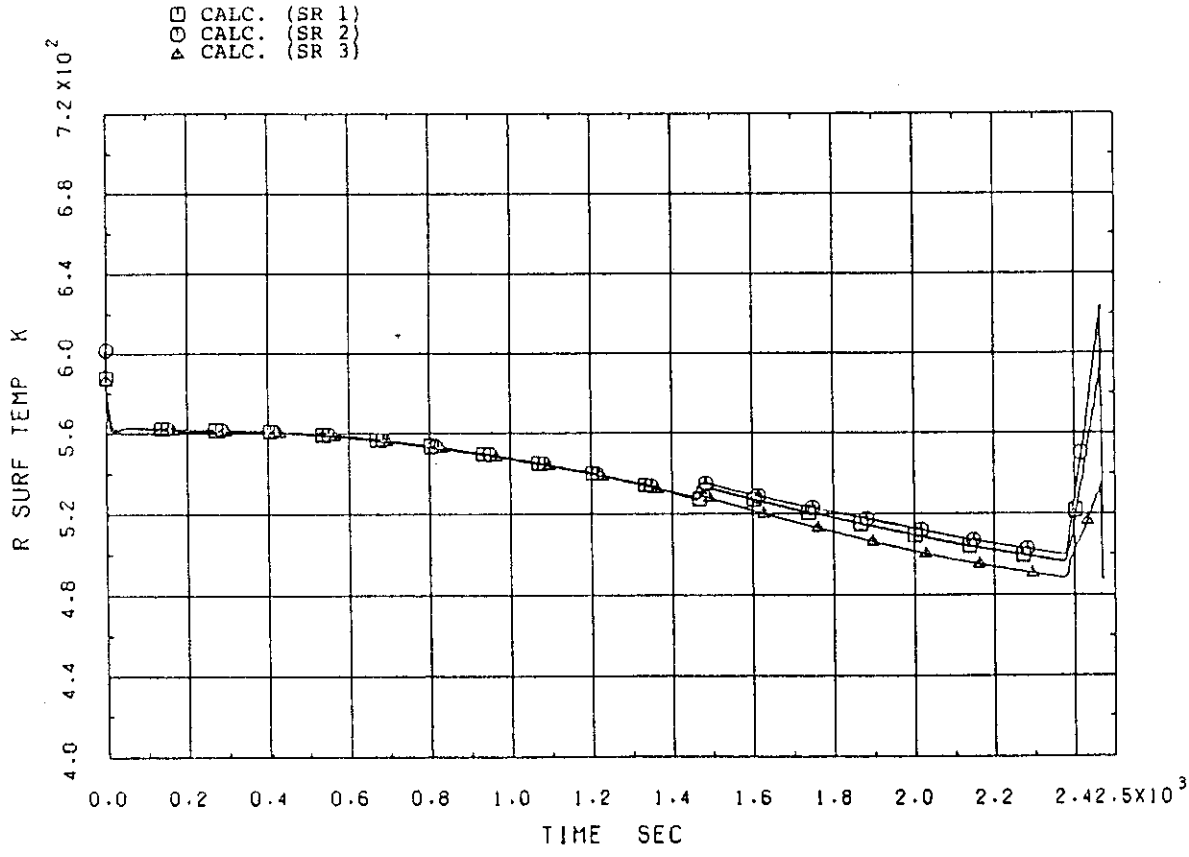

Figure 5.22 Calculated Rod Surface Temperatures

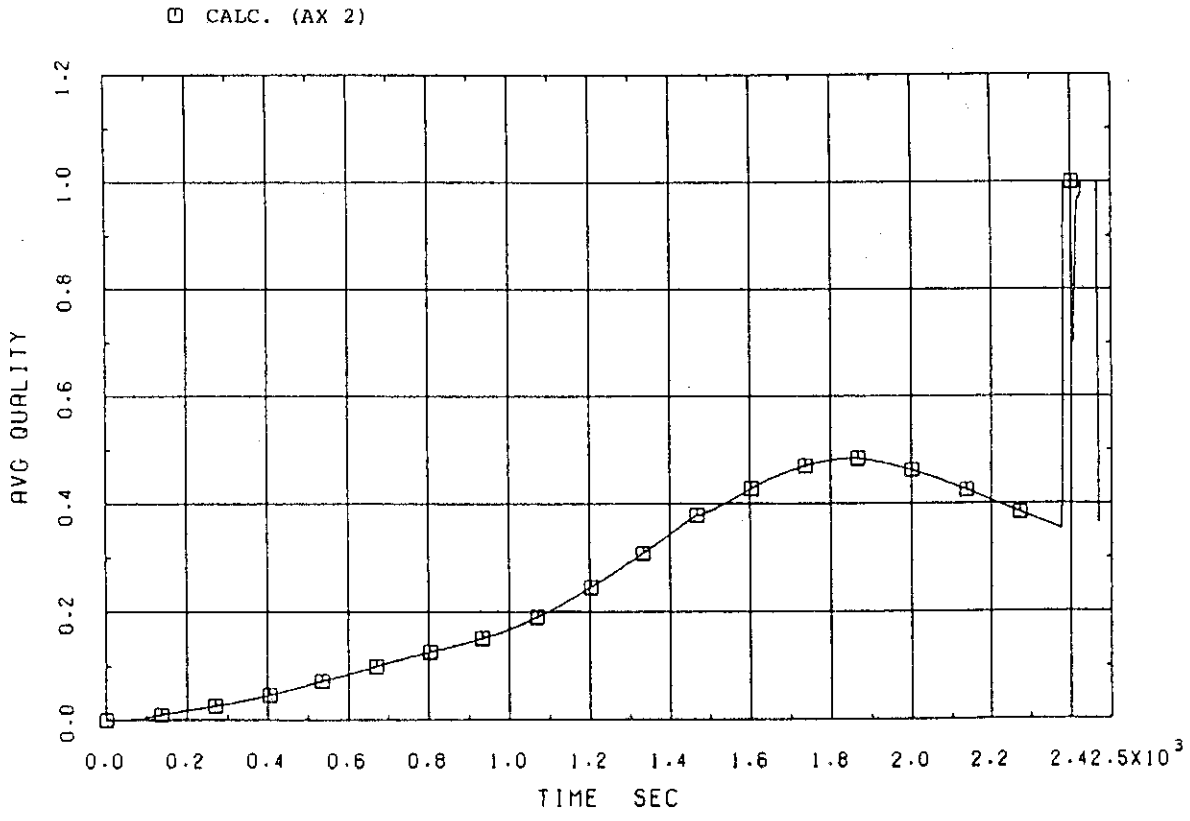

Figure 5.23 Calculated Fluid Quality in the Middle Core

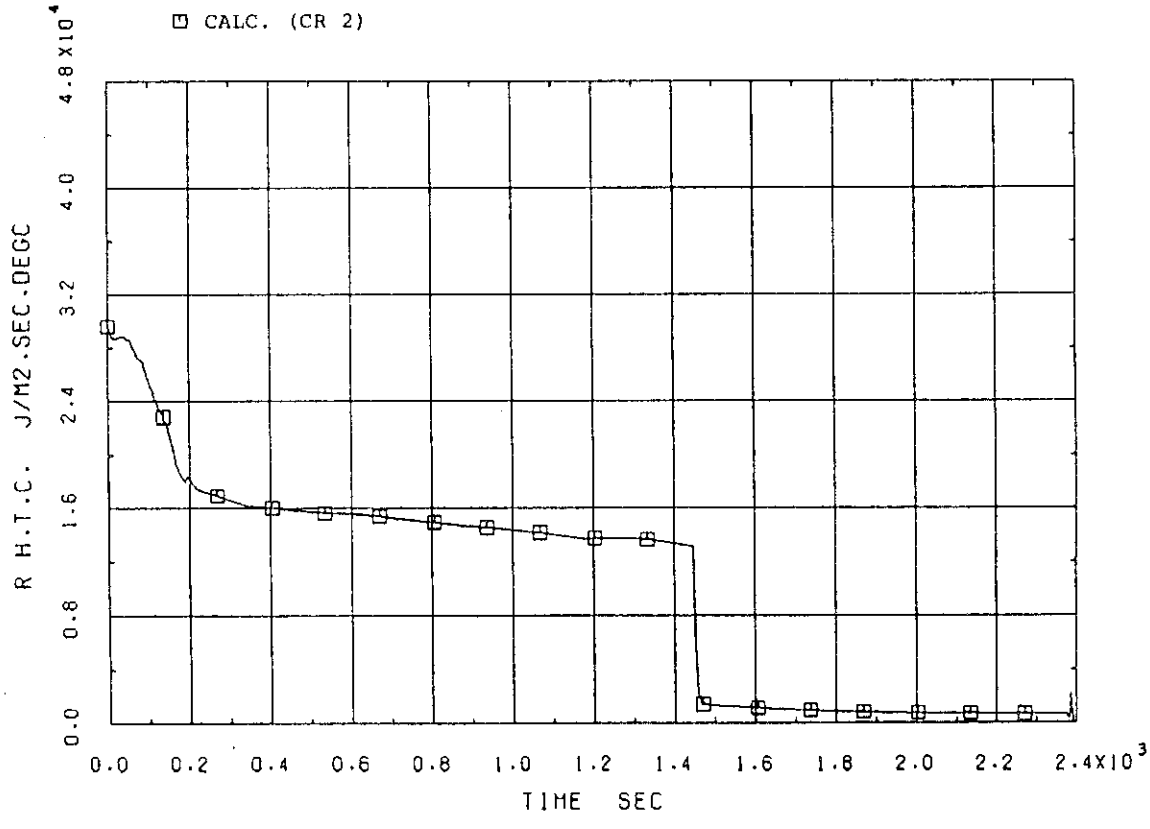

Figure 5.24 Calculated Rod Surface Heat Transfer Coefficient in the Middle Core

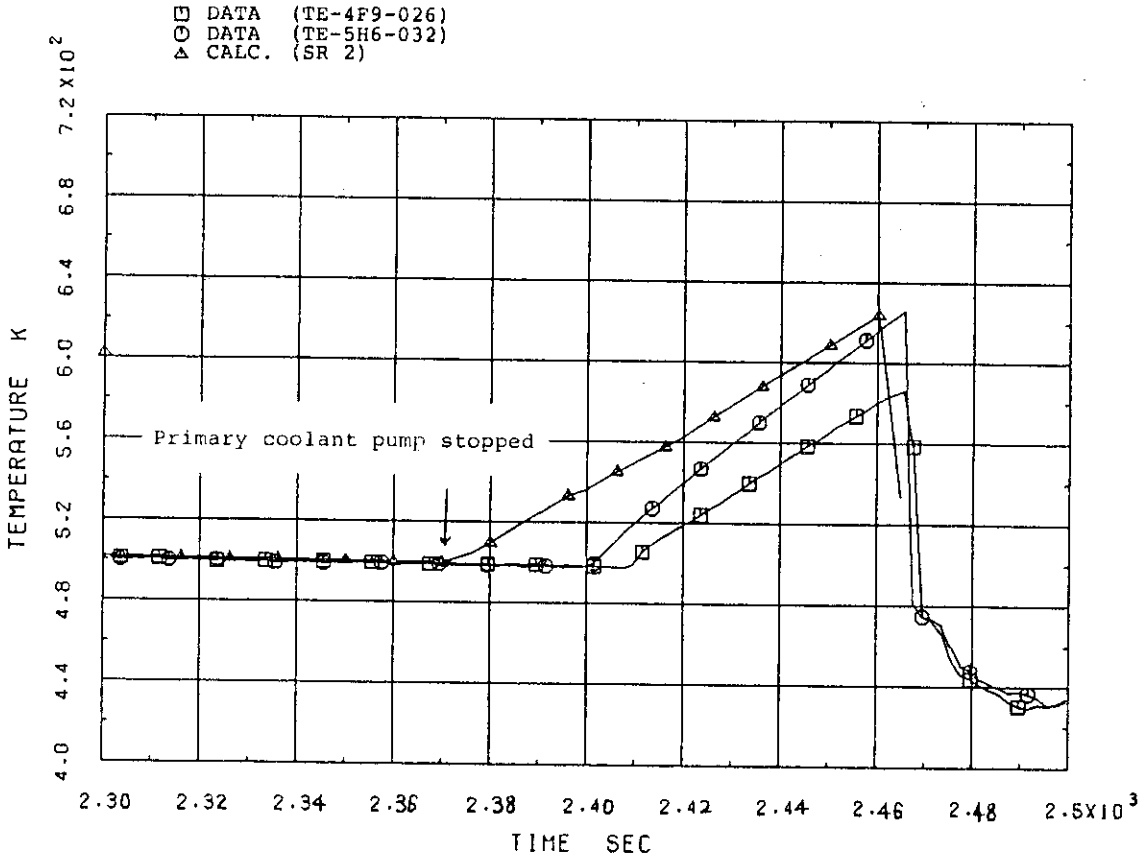

Figure 5.25 Fuel Rod Surface Temperature during L8-1

6. Conclusions

The post-test analysis of LOFT LOCE L3-6/L8-1 by RELAP4/MOD6/U4/J3 was successfully carried out and reasonable agreements between experimental data and calculational results were obtained. Conclusions based on the discussions in Chapter 5 are as follows:

1. The overall primary system behavior dueing the small break LOCA with running primary coolant pumps was able to be simulated by homogeneous equilibrium model and auxiliary flow models in RELAP4/MOD6/U4/J3. An exception was the fluid behavior in the intact loop hot leg where the flow was observed to be stratified.

2. The calculated primary system mass inventory was in good agreement with the data. The agreement was accomplished by using a conventional Henry-Fauske HEM choked break flow model with $C_D = 0.8$. But careful examination will be needed if this value of discharge coefficient and the choked flow model used here can be utilized to simulate the small break LOCA with another size and configuration of break.

3. Primary pump degradation model with the tabular two-phase characteristic data, which had been reported by INEL as the RELAP4/MOD6's input data[4], seemed to be insufficient to predict the differential pressure in the intact loop.

4. Fluid distribution inside the reactor vessel during the most latest portion of LOCE L3-6 could not be simulted well. Calculated results showed too much accumulation of liquid in the upper plenum and it made core fluid condition more severe than the data. As a result, the temperature excusion of fuel rods started earlier in the calculation than the data. Two-phase fluid flow model under the high-void condition should be improved.

5. The calculated pressure and temperature in the steam generator secondary were showing different tendency from the data. The main cause of discrepancy was over-estimation of heat transfer in the steam generator.

6. Steam generators liquid level calculation was affected by improper treatment of thermal non-equilibrium inside the steam generator secondary. It needs more detailed nodalization and also more comprehensive measured data to improve the simulation of secondary system responses.

References

(1) K. Yoshida et al., "RELAP4/Mod6/U4/J3: A JAERI Improved Version of RELAP4/MOD6 for Transient Thermal-Hydraulic Analysis of LWR Including Effects of BWR Core Spray", JAERI-M 9394, March 1981.

(2) P.D. Bayless and J.M. Carpenter, "Experimental Data Report for LOFT Nuclear Small Break Experiment L3-6 and Severe Core Transient Experiment L8-1", NUREG/CR-1868, EGG-2075, Jan. 1981.

(3) S.R. Risher et al., "RELAP4/MOD6: A computer Program for Transient Thermal-Hydraulic Analysis of Nuclear Reactor and Related Systems: User's Manual", CDAP-TR-003, Jan. 1978.

(4) E.J. Kee et al., "Best Estimate Prediction for LOFT Nuclear Experiment L3-2", EGG-LOFT-5089, Feb. 1980.

(5) R. Scott Semken, "LOFT Experimental Operating Specification Small Break Test Series L3 Severe Core Transient Test Series L8 Nuclear Tests L3-6 and L8-1", EGG-LOFT-5293, Dec. 1980.

(6) Glenn E McCreery, "Quick-Look Report on LOFT Nuclear Experiment L3-6/L8-1", EGG-LOFT-5318 , Dec. 1980.

(7) D.L. Reeder, "LOFT System and Test Description", NUREG/CR-0247, TREE-1208, R2, July 1978.

APPENDIX A System Configuration of LOFT Facility

The Loss-of-Fluid Test (LOFT) facility has been designed to simulate the major components and system responses of a commercial pressurized water reactor (PWR) during a loss-of-coolant accident. The experimental assembly includes five major subsystems which have been instrumented such that system variables can be measured and recorded during a loss-of-coolant experiment. The subsystems include: (a) the reactor vessel, (b) the intact loop, (c)the broken loop, (d) the blowdown suppression system, and (e) the emergency core cooling system (ECCS). The LOFT major components are shown in Figure A.1.

The LOFT reactor vessel has an annular downcomer, a lower plenum, lower core support plates, a nuclear core, and an upper plenum. The downcomer is connected to the cold legs of the intact and broken loops and contains two instrument stalks. The upper plenum is connected to the hot legs of the intact and broken loops. The core contains 1300 unpressurized nuclear fuel rods arranged in five sequare (15 x 15 assemblies) and four triangular (corner) fuel modules, shown in Figure A.2 The center assembly is highly instrumented. Two of the corner and one of the square assemblies are not instrumented. The fuel rods have an active length of 1.67m and an outside diameter of 10.72 mm.

The fuel consists of UO_2 sintered pellets with an average enrichment of 4.0 wt% fissile uranium (^{235}U) and with a density that is 93 % of theoretical density. The fuel pellet diameter and length are 9.29 and 15.24 mm, respectively. Both ends of the pellets are dished with the total dish volume equal to 2 % of the pellet volume. The cladding inside and outside diameters are 9.48 and 10.72 mm, respectively.

The intact loop simulates three loops of a commercial four-loop PWR and contains a steam generator, two primary coolant pumps in parallel, a pressurizer, a venturi flow meter, and connecting piping. The break location for Experiment L3-6/L8-1 is in the cold leg of the intact loop between the primary coolant pumps and the reactor vessel. The break orifice is in a pipe that connects the intact loop cold leg to the blowdown suppression tank (BST).

The broken loop consists of a hot leg and cold leg that are connected to the reactor vessel and the BST header. Each leg consists of a break plane orifice, a quick-opening blowdown valve (QORV), a recir-

culation line, an isolation valve, and connecting piping. The recirculation lines establish a small flow from the broken loop to the intact loop and are used to warm up the broken loop. In this experiment the QOBVs and isolation valves remained closed, as the break was in the intact loop cold leg. The broken loop hot leg also contains a simulated steam generator and simulated pump. These simulators have hydraulic orifice plate assemblies which have similar (passive) resistances to flow as an active steam generator and pump.

The blowdown suppression system is comprised of the BST header, the BST, the nitrogen pressurization system, and the BST spray system. The blowdown header is connected to the suppression tank downcomers which extend inside the tank below the water level. The header is also directly connected to the BST vapor space to allow pressure equilibration. The nitrogen pressurization system is supplied by the LOFT inert gas system and uses a remote controlled pressure regulator to establish and maintain the specified BST initial pressure. The spray system consists of a centrifugal pump that discharges through a heatup exchanger and any of three spray header or a pump recirculation line that contains a cooldown heat exchanger. The spray pump suction can be aligned to either the BST or the borated water storage tank. The three spray headers have flow rate capacities of 1.3, 3.8, and 13.9 L/s, respectively, and located in the BST along the upper centerline. For Experiment L3-6/ L8-1, the BST header was not used to carry flow. Break flow entered the BST via a 4 inches pipe which was connected to the end of the BST and discharged below the water level. The BST spray pump suction was connected to the BST and the liquid in the BST was recirculated at full spray pump capacity.

The LOFT ECCS simulates the ECCS of a commercial PWR. It consists of two accumulators, a high-pressure injection system (HPIS), and a low-pressure injection system (LPIS). Each system is arranged to inject scaled flow rates of emergency core coolant directly into the primary coolant system. During Experiment L3-6, the accumulators were not used, and HPIS flow was directed to the reactor downcomer. During the reflood portion of Experiment L8-1, both HPIS pumps and one accumulator injected unscaled coolant flow into the reactor vassel downcomer. The LPIS pumps were not used.

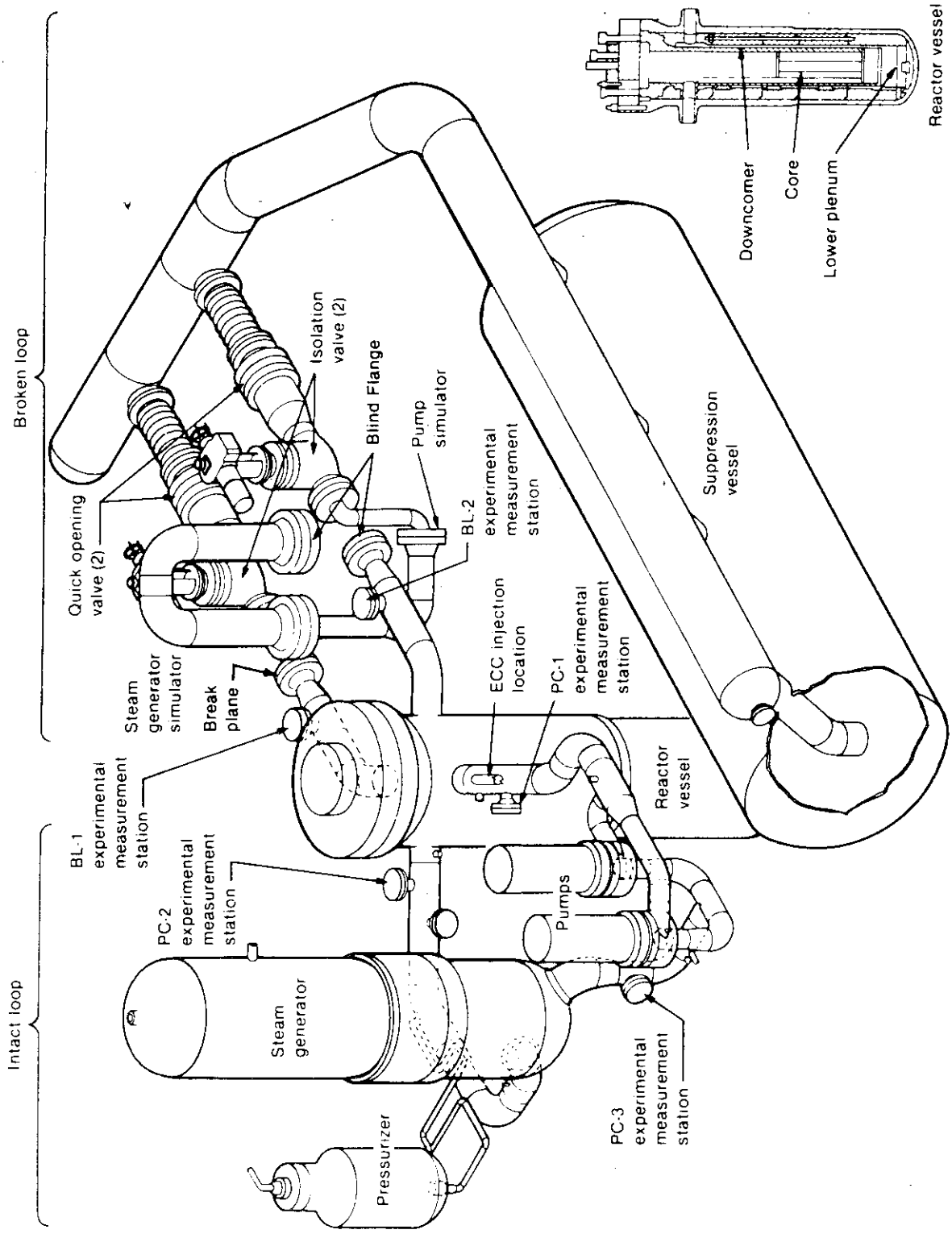

Figure A.1 LOFT Major Components